Electronic Supplementary Material (ESI) for Physical Chemistry Chemical Physics.

The role of electron-nuclear coupling on multi-state photoelectron spectra, scattering processes and phase transitions

Joy Dutta[1], Soumya Mukherjee[1], Koushik Naskar, Sandip Ghosh, Bijit Mukherjee, Satyam Ravi and Satrajit Adhikari*

School of Chemical Sciences, Indian Association for the Cultivation of Science, Jadavpur, Kolkata - 700032, India

Electronic Supplementary Information

*Author for correspondence: e-mail: pcsa@iacs.res.in

[1]J. Dutta and S. Mukherjee contributed equally to this work

S1 Born-Oppenheimer Treatment

One can start the formulation of Born-Oppenheimer (BO) treatment[1] with time-independent molecular Schrödinger equation (SE):

$$\hat{H}(\mathbf{r},\mathbf{R})\Psi(\mathbf{r},\mathbf{R}) = E\Psi(\mathbf{r},\mathbf{R}), \tag{S1}$$

where the electronic and nuclear coordinate vectors are collectively symbolized as $\mathbf{r}$ and $\mathbf{R}$, respectively. The total molecular Hamiltonian, $\hat{H}(\mathbf{r},\mathbf{R})$ is composed of nuclear kinetic energy operator $[\hat{T}_{\text{nuc}}(\mathbf{R})]$ and electronic Hamiltonian $[\hat{H}_{\text{el}}(\mathbf{r};\mathbf{R})]$:

$$\hat{H}(\mathbf{r},\mathbf{R}) = \hat{T}_{\text{nuc}}(\mathbf{R}) + \hat{H}_{\text{el}}(\mathbf{r};\mathbf{R}), \tag{S2}$$

where

$$\hat{T}_{\text{nuc}}(\mathbf{R}) = \sum \frac{1}{2M}\hat{P}^2 = -\sum \frac{\hbar^2}{2M}\left(\frac{\partial^2}{\partial \mathbf{R}^2}\right), \tag{S3}$$

with $\hat{P}$ represents nuclear momenta. On the other hand, the electronic Hamiltonian can be expressed as,

$$\hat{H}_{\text{el}}(\mathbf{r};\mathbf{R}) = \hat{T}_{\text{el}}(\mathbf{r}) + \hat{U}_{coul}(\mathbf{r};\mathbf{R}), \tag{S4}$$

where $\hat{U}_{coul}(\mathbf{r};\mathbf{R})$ is total Coulomb energy due to interaction among nuclei and electrons. $\hat{T}_{\text{el}}(\mathbf{r})$ presents the kinetic energy of electrons:

$$\hat{T}_{\text{el}}(\mathbf{r}) = \sum \frac{1}{2m_e}\hat{p}^2 = -\sum \frac{\hbar^2}{2m_e}\left(\frac{\partial^2}{\partial \mathbf{r}^2}\right), \tag{S5}$$

where $\hat{p}$ indicates electronic momenta. The electronic eigenfunction $[\xi_i(\mathbf{r};\mathbf{R})]$ for any state (i^{th}) is parametrically dependent on nuclear coordinate $(\mathbf{R})$ and satisfy the following time independent electronic SE,

$$\hat{H}_{\text{el}}(\mathbf{r};\mathbf{R})\xi_i(\mathbf{r};\mathbf{R}) = u_i(\mathbf{R})\xi_i(\mathbf{r};\mathbf{R}). \tag{S6}$$

Owing to the large mass difference between electrons (m_e) and nuclei (M), the electronic Hamiltonian $[\hat{H}_{\text{el}}(\mathbf{r};\mathbf{R})]$ is assumed as the zeroth order Hamiltonian, $\hat{H}_0(\mathbf{r};\mathbf{R})$, where $\hat{T}_{\text{nuc}}(\mathbf{R})$ (see Eq. S3) can be considered as a perturbation on $\hat{H}_0(\mathbf{r};\mathbf{R})$:

$$\hat{H}(\mathbf{r},\mathbf{R}) = \hat{H}_{\text{el}}(\mathbf{r};\mathbf{R}) + \hat{T}_{\text{nuc}}(\mathbf{R}) = \hat{H}_0(\mathbf{r};\mathbf{R}) + \hat{T}_{\text{nuc}}(\mathbf{R}) \tag{S7}$$

Considering the quantity $\left(\frac{m_e}{M_0}\right)^{1/4}$ (M_0 is the mean nuclear mass) as the switching parameter, κ, the nuclear kinetic energy operator can be redefined as,

$$\hat{T}_{\text{nuc}}(\mathbf{R}) = \kappa^4 \hat{H}_1(\mathbf{R}), \tag{S8}$$

where

$$\hat{H}_1(\mathbf{R}) = -\sum \left(\frac{M_0}{M}\right)\left(\frac{\hbar^2}{2m_e}\right)\left(\frac{\partial^2}{\partial \mathbf{R}^2}\right) \tag{S9}$$

and thereby, total Hamiltonian turns into,

$$\hat{H}(\mathbf{r},\mathbf{R}) = \hat{H}_0(\mathbf{r};\mathbf{R}) + \kappa^4 \hat{H}_1(\mathbf{R}). \tag{S10}$$

On the other hand, if we take a nuclear geometry $\mathbf{R}$ very close to $\mathbf{R}^0$ [$\kappa\mathbf{x}\,(=\mathbf{R}-\mathbf{R}^0)$ denotes deviation in nuclear coordinate from reference geometry], the eigenfunctions (ξ_i) and the eigenvalues (u_i) of the electronic Hamiltonian as depicted in Eq. S6 can be expanded in Taylor series around $\mathbf{R}^0$:

$$u_i(\mathbf{R}) = u_i(\mathbf{R}^0 + \kappa\mathbf{x}) = u_i^{(0)}(\mathbf{R}^0) + \kappa u_i^{(1)}(\mathbf{x}) + \kappa^2 u_i^{(2)}(\mathbf{x}) + ... \tag{S11}$$

$$\xi_i(\mathbf{r};\mathbf{R}) = \xi_i(\mathbf{r};\mathbf{R}^0 + \kappa\mathbf{x}) = \xi_i^{(0)}(\mathbf{r};\mathbf{R}^0) + \kappa\xi_i^{(1)}(\mathbf{r};\mathbf{x}) + \kappa^2\xi_i^{(2)}(\mathbf{r};\mathbf{x}) + ... \tag{S12}$$

Similarly, the zeroth order electronic Hamiltonian [$\hat{H}_0\,(\mathbf{r};\mathbf{R})$ in Eq. S10] is also expanded around the same nuclear configuration, $\mathbf{R}^0$:

$$\hat{H}_{el}\,(\mathbf{r};\mathbf{R}) = \hat{H}_0\,(\mathbf{r};\mathbf{R}) = \hat{H}_0\left(\mathbf{r};\mathbf{R}^0 + \kappa\mathbf{x}\right) = \hat{H}_0^{(0)}(\mathbf{r};\mathbf{R}^0) + \kappa\hat{H}_0^{(1)}(\mathbf{r};\mathbf{x}) + \kappa^2\hat{H}_0^{(2)}(\mathbf{r};\mathbf{x}) + ... \tag{S13}$$

While substituting Eqs. S11, S12 and S13 in Eq. S6, we obtain:

$$\left[(\hat{H}_0^{(0)} + \kappa\hat{H}_0^{(1)} + \kappa^2\hat{H}_0^{(2)} + ..) - (u_i^{(0)} + \kappa u_i^{(1)} + \kappa^2 u_i^{(2)} + ..)\right]\left[\xi_i^{(0)} + \kappa\xi_i^{(1)} + \kappa^2\xi_i^{(2)} + ...\right] = 0, \tag{S14}$$

where the functional dependence on $\mathbf{r}$ or/and $\mathbf{R}$ are omitted now onwards. When we compare the terms with zeroth, first and second power of κ, the following relations are obtained,

$$(\hat{H}_0^{(0)} - u_i^{(0)})\xi_i^{(0)} = 0 \tag{S15}$$

$$(\hat{H}_0^{(0)} - u_i^{(0)})\xi_i^{(1)} = -(\hat{H}_0^{(1)} - u_i^{(1)})\xi_i^{(0)} \tag{S16}$$

$$(\hat{H}_0^{(0)} - u_i^{(0)})\xi_i^{(2)} = -(\hat{H}_0^{(1)} - u_i^{(1)})\xi_i^{(1)} - (\hat{H}_0^{(2)} - u_i^{(2)})\xi_i^{(0)} \tag{S17}$$

Such perturbation is employed on the electronic Hamiltonian at a fixed reference geometry [$\hat{H}_0^{(0)}(\mathbf{r};\mathbf{R}^0)$] to get the corrections on eigenvalues and eigenfunctions of $\hat{H}_{el}\,(\mathbf{r};\mathbf{R})$ (see Eqs. S13 to S17).

On the other hand, one can carry out a perturbative approach by applying $\hat{T}_{\rm nuc}(\mathbf{R})$ as follows,

$$\hat{H}(\mathbf{r},\mathbf{R}) = \hat{H}_{el}\,(\mathbf{r};\mathbf{R}) + \hat{T}_{\rm nuc}(\mathbf{R}) \tag{S18}$$

While doing so, we replace $\frac{\partial}{\partial \mathbf{R}} = \frac{1}{\kappa}.\frac{\partial}{\partial \mathbf{x}}$ in Eq. S9 and the nuclear kinetic energy operator is modified as,

$$\hat{T}_{\rm nuc}(\mathbf{x}) = \kappa^2 \hat{H}_1^{(2)}(\mathbf{x}), \tag{S19}$$

with

$$\hat{H}_1^{(2)}(\mathbf{x}) = -\sum \left(\frac{M_0}{M}\right)\left(\frac{\hbar^2}{2m_e}\right)\left(\frac{\partial^2}{\partial \mathbf{x}^2}\right).$$

When the nuclear kinetic energy operator (Eq. S19) and the electronic Hamiltonian (Eq. S13) are substituted in Eq. S18, we arrive the following molecular Hamiltonian,

$$\hat{H}(\mathbf{r},\mathbf{R}) = \hat{H}_{el}\left(\mathbf{r};\mathbf{R}\right) + \hat{T}_{\rm nuc}(\mathbf{R}) = \Big[\hat{H}_0^{(0)}(\mathbf{r};\mathbf{R}^0) + \kappa \hat{H}_0^{(1)}(\mathbf{r};\mathbf{x}) + \kappa^2\{\hat{H}_0^{(2)}(\mathbf{r};\mathbf{x}) + \hat{H}_1^{(2)}(\mathbf{x})\} + ..\Big] \tag{S20}$$

In case of this perturbative approach (see Eq. S20), since $\hat{H}_{el}\left(\mathbf{r};\mathbf{R}\right)$ is also the zeroth order Hamiltonian, the eigenfunction, $\xi_i(\mathbf{r};\mathbf{R})$ $[= \Psi_i^{(0)}(\mathbf{r};\mathbf{R})]$ and eigenvalue $u_i(\mathbf{R})$ $[= U_i^{(0)}(\mathbf{R})]$ can be considered as zeroth order molecular wavefunction and energy, respectively. Hence, one can write,

$$\hat{H}_{el}\left(\mathbf{r};\mathbf{R}\right)\Psi_i^{(0)}(\mathbf{r};\mathbf{R}) = U_i^{(0)}(\mathbf{R})\Psi_i^{(0)}(\mathbf{r};\mathbf{R}). \tag{S21}$$

Consequently, the perturbed molecular SE due to nuclear kinetic energy operator on the i^{th} state will be given by,

$$\hat{H}(\mathbf{r},\mathbf{R})\Psi_i(\mathbf{r},\mathbf{R}) = E_i\Psi_i(\mathbf{r},\mathbf{R}). \tag{S22}$$

Therefore, E_i takes the following form,

$$\begin{aligned} E_i &= U_i^{(0)}(\mathbf{R}) + \kappa U_i^{(1)}(\mathbf{R}) + \kappa^2 U_i^{(2)}(\mathbf{R}) + ... \\ &= [u_i^{(0)}(\mathbf{R}^0) + \kappa u_i^{(1)}(\mathbf{x}) + \kappa^2 u_i^{(2)}(\mathbf{x}) + ...] + \kappa U_i^{(1)}(\mathbf{R}) + \kappa^2 U_i^{(2)}(\mathbf{R}) + ... \text{ (from Eq. } S11\text{)} \\ &= E_i^{(0)}(\mathbf{R}^0) + \kappa E_i^{(1)}(\mathbf{R}) + \kappa^2 E_i^{(2)}(\mathbf{R}) + ... \ , \end{aligned} \tag{S23}$$

where $E_i^{(0)}(\mathbf{R}^0) = u_i^{(0)}(\mathbf{R}^0)$, $E_i^{(1)}(\mathbf{R}) = u_i^{(1)}(\mathbf{x}) + U_i^{(1)}(\mathbf{R})$, $E_i^{(2)}(\mathbf{R}) = u_i^{(2)}(\mathbf{x}) + U_i^{(2)}(\mathbf{R})$, etc. It is important to note that $E_i^{(0)}$ is defined at $\mathbf{R}^0$ and the remaining quantities [$\kappa E_i^{(1)}$, $\kappa^2 E_i^{(2)}$, ...] are functions of $\mathbf{R}$, but finally, the total molecular energy (E_i) should appear as independent of electronic or nuclear coordinates. On the other hand, molecular wavefunction for the i^{th} state $[\Psi_i(\mathbf{r},\mathbf{R})]$ takes the following form:

$$\Psi_i(\mathbf{r},\mathbf{R}) = \Psi_i^{(0)}(\mathbf{r};\mathbf{R}) + \kappa\Psi_i^{(1)}(\mathbf{r},\mathbf{R}) + \kappa^2\Psi_i^{(2)}(\mathbf{r},\mathbf{R}) + ... \tag{S24}$$

due to the perturbation of nuclear kinetic energy operator.

Substituting Eqs. S20, S23 and S24 in Eq. S22, we obtain the molecular SE for i^{th} state in Taylor series,

$$\Big[(\hat{H}_0^{(0)} + \kappa\hat{H}_0^{(1)} + \kappa^2(\hat{H}_0^{(2)} + \hat{H}_1^{(2)}) + ...) - (E_i^{(0)} + \kappa E_i^{(1)} + \kappa^2 E_i^{(2)} + ...)\Big]$$
$$\Big[\Psi_i^{(0)} + \kappa\Psi_i^{(1)} + \kappa^2\Psi_i^{(2)} + ...\Big] = 0 \tag{S25}$$

where the functional dependencies on electronic and nuclear coordinates are omitted. While collecting coefficients of κ^0, κ^1 and κ^2, we obtain:

$$(\hat{H}_0^{(0)} - E_i^{(0)})\Psi_i^{(0)} = 0 \tag{S26}$$

$$(\hat{H}_0^{(0)} - E_i^{(0)})\Psi_i^{(1)} = -(\hat{H}_0^{(1)} - E_i^{(1)})\Psi_i^{(0)} \tag{S27}$$

$$(\hat{H}_0^{(0)} - E_i^{(0)})\Psi_i^{(2)} = -(\hat{H}_0^{(1)} - E_i^{(1)})\Psi_i^{(1)} - (\hat{H}_0^{(2)} + \hat{H}_1^{(2)} - E_i^{(2)})\Psi_i^{(0)} \tag{S28}$$

One can observe that $\xi_i^{(0)}(\mathbf{r};\mathbf{R}^0)$ and $\Psi_i^{(0)}(\mathbf{r};\mathbf{R})$ are eigenfunctions of same Hamiltonian, $\hat{H}_0^{(0)}$ (see Eq. S15 and S26) with same eigenvalue ($u_i^{(0)}$ or $E_i^{(0)}$) and therefore, the following relation can be written,

$$\Psi_i^{(0)}(\mathbf{r};\mathbf{R}) = \psi_i^{(0)}(\mathbf{R})\xi_i^{(0)}(\mathbf{r};\mathbf{R}^0), \tag{S29}$$

where $\psi_i^{(0)}(\mathbf{R})$ is the zeroth order nuclear wavefunction. Similarly, by comparing the two sets of perturbing series (Eqs. S15, S16, S17 and S26, S27, S28), we obtain the first and second order corrections to the i^{th} state molecular wavefunction as presented below,

$$\Psi_i^{(1)}(\mathbf{r},\mathbf{R}) = \psi_i^{(0)}(\mathbf{R})\xi_i^{(1)}(\mathbf{r};\mathbf{x}) + \psi_i^{(1)}(\mathbf{R})\xi_i^{(0)}(\mathbf{r};\mathbf{R}^0) \tag{S30}$$

$$\Psi_i^{(2)}(\mathbf{r},\mathbf{R}) = \psi_i^{(0)}(\mathbf{R})\xi_i^{(2)}(\mathbf{r};\mathbf{x}) + \psi_i^{(1)}(\mathbf{R})\xi_i^{(1)}(\mathbf{r};\mathbf{x}) + \psi_i^{(2)}(\mathbf{R})\xi_i^{(0)}(\mathbf{r};\mathbf{R}^0) \tag{S31}$$

Therefore, molecular wavefunction for the i^{th} state takes the following form,

$$\begin{aligned}
\Psi_i(\mathbf{r},\mathbf{R}) &= \Psi_i^{(0)}(\mathbf{r};\mathbf{R}) + \kappa\Psi_i^{(1)}(\mathbf{r},\mathbf{R}) + \kappa^2\Psi_i^{(2)}(\mathbf{r},\mathbf{R}) + ... \\
&= \psi_i^{(0)}(\mathbf{R})\{\xi_i^{(0)}(\mathbf{r};\mathbf{R}^0) + \kappa\xi_i^{(1)}(\mathbf{r};\mathbf{x}) + \kappa^2\xi_i^{(2)}(\mathbf{r};\mathbf{x}) + ...\} + \\
&\quad \kappa\psi_i^{(1)}(\mathbf{R})\{\xi_i^{(0)}(\mathbf{r};\mathbf{R}^0) + \kappa\xi_i^{(1)}(\mathbf{r};\mathbf{x}) + ...\} + \\
&\quad \kappa^2\psi_i^{(2)}(\mathbf{R})\{\xi_i^{(0)}(\mathbf{r};\mathbf{R}^0) + ...\} + ... \\
&= \{\psi_i^{(0)}(\mathbf{R}) + \kappa\psi_i^{(1)}(\mathbf{R}) + \kappa^2\psi_i^{(2)}(\mathbf{R}) + ...\} \\
&\quad \{\xi_i^{(0)}(\mathbf{r};\mathbf{R}^0) + \kappa\xi_i^{(1)}(\mathbf{r};\mathbf{x}) + \kappa^2\xi_i^{(2)}(\mathbf{r};\mathbf{x}) + ...\} \\
&= \psi_i^{\mathrm{ad}}(\mathbf{R})\xi_i^{\mathrm{ad}}(\mathbf{r};\mathbf{R})
\end{aligned} \tag{S32}$$

Therefore, when we consider upto the second order correction (i.e., κ^4), total molecular wavefunction can be written as a product of adiabatic nuclear wavefunction and electronic eigenfunction.

On the other hand, the third order correction to the molecular wavefunction takes the following form,

$$\begin{aligned}\Psi_i^{(3)} &= \psi_i^{(0)}(\mathbf{R})\xi_i^{(3)}(\mathbf{r};\mathbf{x}) + \psi_i^{(1)}(\mathbf{R})\xi_i^{(2)}(\mathbf{r};\mathbf{x}) + \psi_i^{(2)}(\mathbf{R})\xi_i^{(1)}(\mathbf{r};\mathbf{x}) + \psi_i^{(3)}(\mathbf{R})\xi_i^{(0)}(\mathbf{r};\mathbf{R}^0) \\ &\quad + F(\mathbf{r},\mathbf{x}), \end{aligned} \tag{S33}$$

where the term, $F(\mathbf{r},\mathbf{x})$ is the solution of the following inhomogeneous equation:

$$(\hat{H}_0^{(0)} - E_i^{(0)})F(\mathbf{r},\mathbf{x}) = \frac{\hbar^2}{m_e}\sum\Big(\frac{M_0}{M}\Big)\Big(\frac{\partial\psi_i^{(0)}(\mathbf{R})}{\partial\mathbf{x}}\Big)\Big(\frac{\partial\xi_i^{(1)}(\mathbf{r};\mathbf{x})}{\partial\mathbf{x}}\Big) \tag{S34}$$

Again, the fourth order correction is presented as,

$$\begin{aligned}\Psi_i^{(4)} &= \psi_i^{(0)}(\mathbf{R})\xi_i^{(4)}(\mathbf{r};\mathbf{x}) + \psi_i^{(1)}(\mathbf{R})\xi_i^{(3)}(\mathbf{r};\mathbf{x}) + \psi_i^{(2)}(\mathbf{R})\xi_i^{(2)}(\mathbf{r};\mathbf{x}) + \psi_i^{(3)}(\mathbf{R})\xi_i^{(1)}(\mathbf{r};\mathbf{x}) + \psi_i^{(4)}(\mathbf{R})\xi_i^{(0)}(\mathbf{r};\mathbf{R}^0) \\ &\quad + G(\mathbf{r},\mathbf{x}). \end{aligned} \tag{S35}$$

Here also the term, $G(\mathbf{r},\mathbf{x})$ is the solution of the following equation:

$$\begin{aligned}(\hat{H}_0^{(0)} - E_i^{(0)})G(\mathbf{r},\mathbf{x}) &= -H_0^{(1)}F(\mathbf{r},\mathbf{x}) - C\psi_i^{(0)}(\mathbf{R})\xi_i^{(0)}(\mathbf{r};\mathbf{R}^0) - (H_1^{(2)} + u_i^{(2)} - E_i^2)[\psi_i^{(0)}(\mathbf{R})\xi_i^{(2)}(\mathbf{r};\mathbf{x}) \\ &\quad + \psi_i^{(1)}(\mathbf{R})\xi_i^{(1)}(\mathbf{r};\mathbf{x})] - (u_i^{(3)} - E_i^{(3)})\psi_i^{(0)}(\mathbf{R})\xi_i^{(1)}(\mathbf{r};\mathbf{x}), \end{aligned} \tag{S36}$$

where the constant, C takes the following form,

$$C = \frac{\hbar^2}{2m_e}\sum\Big(\frac{M_0}{M}\Big)\int \xi_i^{(0)}(\mathbf{r};\mathbf{R}^0)\frac{\partial^2}{\partial\mathbf{x}^2}\xi_i^{(2)}(\mathbf{r};\mathbf{x})d\mathbf{r} \tag{S37}$$

It is clearly evident from Eqs. S33 and S35 that the third and fourth order corrections on molecular wavefunctions contain the nuclear derivative coupling terms [$F(\mathbf{r},\mathbf{x})$ and $G(\mathbf{r},\mathbf{x})$] over the electronic eigenfunctions, where such quantities cannot be written in the multiplicative form, $\psi_i^{(m)}(\mathbf{R})\xi_i^{(n)}(\mathbf{r};\mathbf{x})$. Indeed, if we neglect $F(\mathbf{r},\mathbf{x})$ and $G(\mathbf{r},\mathbf{x})$ considering those terms being associated with the switching parameters κ^6 and κ^8, respectively, in the following form, we can revive the product form of molecular wavefunction corrected upto κ^8 for the i^{th} state as shown in Eq. S32:

$$\begin{aligned}\Psi_i(\mathbf{r},\mathbf{R}) &= \{\psi_i^{(0)}(\mathbf{R}) + \kappa\psi_i^{(1)}(\mathbf{R}) + \kappa^2\psi_i^{(2)}(\mathbf{R}) + \kappa^3\psi_i^{(3)}(\mathbf{R}) + \kappa^4\psi_i^{(4)}(\mathbf{R})\ldots\ldots\} \\ &\quad \{\xi_i^{(0)}(\mathbf{r};\mathbf{R}^0) + \kappa\xi_i^{(1)}(\mathbf{r};\mathbf{x}) + \kappa^2\xi_i^{(2)}(\mathbf{r};\mathbf{x}) + \kappa^3\xi_i^{(3)}(\mathbf{r};\mathbf{x}) + \kappa^4\xi_i^{(4)}(\mathbf{r};\mathbf{x})\ldots..\} \\ &= \psi_i^{\mathrm{ad}}(\mathbf{R})\xi_i^{\mathrm{ad}}(\mathbf{r};\mathbf{R}) \end{aligned} \tag{S38}$$

On the contrary, such derivative coupling terms, [$F(\mathbf{r},\mathbf{x})$ and $G(\mathbf{r},\mathbf{x})$] naturally appear as the nuclear kinetic energy operator acts on the product form of molecular wavefunction, where the electronic eigenfunctions are projected out to formulate nuclear SE. While formulating such nuclear SE in terms of nonadiabatic coupling terms (NACTs), one needs to consider the Born-Oppeneheimer-Huang (BOH) expansion of the molecular wavefunction [$\Psi(\mathbf{r},\mathbf{R}) = \sum_{i=1}^{N} \Psi_i(\mathbf{r},\mathbf{R}) = \sum_{i=1}^{N} \psi_i^{\mathrm{ad}}(\mathbf{R})\ \xi_i^{\mathrm{ad}}(\mathbf{r};\mathbf{R})$][2] so that the couplings among all possible electronic states are incorporated.

S2 Degenerate Perturbation Theory: linear Jahn-Teller (JT) Model

According to the "toy" model of linear JT coupling,[3] total electron-nuclear Hamiltonian can be represented as,

$$\hat{H} = \hat{H}^0 + \hat{W}, \tag{S39}$$

where $\hat{H}^0$ can be segregated into nuclear kinetic energy operator ($\hat{T}_{\mathrm{nuc}}$) and the unperturbed potential energy surfaces ($\hat{U}_0$) matrices. According to JT theorem,[3] any non-linear molecule having degenerate electronic states encounters distortion and removes the degeneracy in order to lower the energy of the system. We consider the nuclear vibrations along x and y coordinates as simple 2D harmonic oscillators and arrive the following form of $\hat{U}_0$ for doubly degenerate electronic states,

$$\hat{U}_0 = \frac{\omega}{2}\begin{pmatrix} x^2+y^2 & 0 \\ 0 & x^2+y^2 \end{pmatrix} \tag{S40}$$

where ω depicts the angular frequency of those vibrations. On the other hand, linear JT perturbation can be defined as:

$$\hat{W} = k\begin{pmatrix} y & x \\ x & -y \end{pmatrix}, \tag{S41}$$

where $x = \rho\cos\phi$ and $y = \rho\sin\phi$ (ρ and ϕ are the polar analogues). We can evaluate the first order corrections to energy with the help of degenerate perturbation theory, which is briefly discussed here below:

For a set of m-fold degenerate states of energy eigenvalue, $E_n^{(0)}$, the set of unperturbed SE is represented as:

$$\hat{H}^0\xi_n^{(0)} = E_n^{(0)}\xi_n^{(0)}, \qquad 1 \le n \le m \tag{S42}$$

While applying a perturbation, the new set appears as:

$$\hat{H}\xi_n \;=\; E_n\xi_n, \qquad 1 \leq n \leq m, \tag{S43}$$

where $\hat{H}$ can be partitioned into two terms, $\hat{H}^0$ and $\lambda\hat{V}$. The second one ($\lambda\hat{V}$) defines the perturbation, where λ represents the switching parameter. While applying the degenerate perturbation theory, we obtain the following secular determinant:

$$\begin{vmatrix} V_{11} - E_n^{(1)} & V_{12} & \cdots & V_{1m} \\ V_{21} & V_{22} - E_n^{(1)} & \cdots & V_{2m} \\ \vdots & \vdots & \ddots & \vdots \\ V_{m1} & V_{m2} & \cdots & V_{mm} - E_n^{(1)} \end{vmatrix} = 0, \qquad 1 \leq n \leq m, \tag{S44}$$

where $V_{ij} = \langle\xi_i^{(0)}|\hat{V}|\xi_j^{(0)}\rangle$ and the m number of roots, $E_1^{(1)}, E_2^{(1)}, ..., E_m^{(1)}$ give the first order corrections to energy.

In case of a doubly degenerate system, the above determinant (Eq. S44) takes the following form:

$$\begin{vmatrix} V_{11} - E_n^{(1)} & V_{12} \\ V_{21} & V_{22} - E_n^{(1)} \end{vmatrix} = 0 \qquad n = 1, 2, \tag{S45}$$

and the two roots appear as:

$$E_{\pm}^{(1)} = \frac{1}{2}\left[V_{11} + V_{22} \pm \sqrt{(V_{11} - V_{22})^2 + 4|V_{12}|^2}\right] \tag{S46}$$

Comparing Eqs. S41 with S45, we find $V_{11} = ky$, $V_{22} = -ky$ and $V_{12} = V_{21} = kx$, which leads to the eigenvalue, $E_{\pm}^{(1)} (= \pm k\sqrt{x^2 + y^2} = \pm k\rho)$. On the other hand, the eigenvectors take the following form:

$$\phi_1 = \begin{pmatrix} \cos\frac{\phi}{2} \\ \sin\frac{\phi}{2} \end{pmatrix} \qquad \phi_2 = \begin{pmatrix} -\sin\frac{\phi}{2} \\ \cos\frac{\phi}{2} \end{pmatrix} \tag{S47}$$

The above mentioned linear JT model was extensively studied by Öpik and Pryce[4] on a hexa aquocupric ion complex $[Cu(NH_4)_2\ (SO_4)_2.6H_2O]$ almost a six decades ago. In this transition metal complex, one can observe crystal field splitting of ^2D state of free copper ion (d^9) in presence of cubic symmetry (t_{2g} and e_g). Öpik *et al.*[4] applied a linear JT perturbation on those degenerate e_g states by doubly degenerate Q_2 and Q_3 vibrational modes. Such phenomenon can be defined by the following potential energy operator:

$$\begin{aligned}\hat{V} &= \hat{U}_0 + \hat{W} \\ &= \frac{1}{2}M{\omega_{\text{b\_vib}}}^2(Q_2^2+Q_3^2)I + A\begin{pmatrix}-Q_3 & -Q_2\\ -Q_2 & Q_3\end{pmatrix},\end{aligned} \tag{S48}$$

where I is 2×2 unit matrix, A represents linear JT term, M is the mass of a corner atom, and $\omega_{\text{b\_vib}}$ denotes the vibrational frequency. As a result of the linear JT perturbation ($\hat{W}$), the two adiabatic potential energy surfaces (APESs) take the following functional form:

$$V_{\pm} = \pm A\rho + \frac{1}{2}M{\omega_{\text{b\_vib}}}^2\rho^2, \tag{S49}$$

where $\rho\,(=\sqrt{Q_2^2+Q_3^2})$ and $\phi\,(=\tan^{-1}\left(\frac{Q_2}{Q_3}\right))$ are the polar analogues of Q_2 and Q_3. It may be noted that the lower APES has the shape of a 'Mexican hat'. The associated electronic wavefunctions to the lower and upper sheets of the PES can be written as:

$$\begin{aligned}\psi_+(\phi) &= \cos\frac{\phi}{2}\left|x^2-y^2\right\rangle + \sin\frac{\phi}{2}\left|3z^2-r^2\right\rangle \\ \psi_-(\phi) &= -\sin\frac{\phi}{2}\left|x^2-y^2\right\rangle + \cos\frac{\phi}{2}\left|3z^2-r^2\right\rangle.\end{aligned} \tag{S50}$$

In the above expression, $|x^2-y^2\rangle$ and $|3z^2-r^2\rangle$ are the eigenfunctions of $d_{x^2-y^2}$ and d_{z^2} orbitals, respectively.

S2.1 The SEs for lower and upper sheet of APES

Under the action of elliptical perturbation[5], $H'(=2A\rho\cos(2\theta-\phi))$: (i) Electronic degeneracy of E_g state is removed with eigenvalues, $\pm A\rho$, accompanied by the formation of a doubly branched APES; (ii) Moreover, selection rule states that two vibrational levels within same electronic state ($j=\pm1$) interact in such a way that pseudo - rotational quantum numbers, 'l's remain as conserved, i.e., levels with same value of $l(=m+\frac{1}{2}j)$ would be coupled with each other; (iii) Consequently, the total vibronic wavefunction can be written in the following form within beyond adiabatic approximation:[5]

$$\Psi = \chi_-(\rho,\phi)\psi_-(\theta) + \chi_+(\rho,\phi)\psi_+(\theta), \tag{S51}$$

where $\chi_\pm$ and $\psi_\pm$ are the nuclear (doubly degenerate e_g vibrations) and electronic (single electron in a ring) wavefunctions, respectively.

Incorporating the vibronic wavefunction, Ψ (Eq. (S51)) and elliptical perturbation ($H' = 2A\rho\cos(2\theta - \phi)$) in time independent Schrödinger Equation (SE), followed by integrating out the electronic coordinate (θ), the two coupled nuclear SEs (belonging to electronic state $j = \pm 1$) are obtained[5] as follows:

$$\begin{bmatrix} H_0 - E & A\rho e^{-i\phi} \\ A\rho e^{i\phi} & H_0 - E \end{bmatrix} \begin{bmatrix} \chi_+ \\ \chi_- \end{bmatrix} = 0, \tag{S52}$$

where H_0 is the unperturbed two dimensional (2D) isotropic harmonic oscillator (IHO) Hamiltonian representing Q_2-Q_3 degenerate (e_g) pair of normal modes and $\chi_\pm$ are defined in terms of radial ($\tau_l^\pm$) and angular ($e^{i\left(l\pm\frac{1}{2}j\right)\phi}$) solutions of 2D IHO interacting with $j = -1$ and $j = +1$ electronic states. After plugging such vibronic eigenfunctions in Eq. (S52), subtraction and addition of resultant differential equations lead to the following expressions[5]:

$$(H_l - A\rho - E)u_g(\rho) = (-1)^{l-\frac{1}{2}}\left(\frac{\hbar^2 l}{2M\rho^2}\right)u_e(\rho), \tag{S53}$$

and

$$(H_l + A\rho - E)\,u_e(\rho) = (-1)^{-(l-\frac{1}{2})}\left(\frac{\hbar^2 l}{2M\rho^2}\right)u_g(\rho), \tag{S54}$$

where $u_g(\rho) = (-1)^{l-\frac{1}{2}}\{\tau_l^+(\rho) - \tau_l^-(\rho)\}$, $u_e(\rho) = \{\tau_l^+(\rho) + \tau_l^-(\rho)\}$ and H_l is defined as:

$$H_l = \frac{\hbar^2}{2M}\left[-\frac{d^2}{d\rho^2} - \frac{1}{\rho}\frac{d}{d\rho} + \frac{l^2 + \frac{1}{4}}{\rho^2}\right] + \frac{1}{2}M\omega_{b\_vib}^2\rho^2. \tag{S55}$$

Using Eqs. (S53), (S54) and (S55), the SEs for ground and excited electronic state are expressed in the respective cases as:

(i) The ground state SE

Since the ground state minima are quite far away from the centre of APES, the right hand side of the Eq. (S53) vanishes for low energy situation and thereby, leading to the following form of radial and total vibronic SE[5]:

$$-\frac{\hbar^2}{2M}\left[\frac{d^2\psi_g(\rho)}{d\rho^2} - \frac{l^2}{\rho^2}\psi_g(\rho)\right] - E^g\psi_g(\rho) + \left(-A\rho + \frac{1}{2}M\omega_{\text{b\_vib}}^2\rho^2\right)\psi_g(\rho) = 0 \qquad \text{radial SE} \tag{S56}$$

and

$$-\frac{\hbar^2}{2M}\left[\frac{\partial^2\chi_g}{\partial\rho^2}+\frac{1}{\rho^2}\frac{\partial^2\chi_g}{\partial\phi^2}\right]-E^g\chi_g+\left(-A\rho+\frac{1}{2}M\omega_{\text{b\_vib}}^2\rho^2\right)\chi_g=0, \qquad \text{total SE} \tag{S57}$$

where $\psi_g(\rho)=\rho^{1/2}u_g(\rho)$ and $\chi_g=\psi_g(\rho)e^{il\phi}$. Furthermore, using the analytic forms of $\chi_\pm$, $\psi_g(\rho)$ and $u_g(\rho)$ as shown above, χ_g can be written as follows[5,6]:

$$\chi_g \;=\; \sqrt{\rho}\,(-1)^{l-\frac{1}{2}}\left\{\chi_+e^{i\phi/2}-\chi_-e^{-i\phi/2}\right\}. \tag{S58}$$

(ii) The excited state SE

In case of high energy situation, the term $u_g(\rho)$ in the Eq. (S54) vanishes, and consequently radial and total SE for upper sheet of PES turn as[5]:

$$-\frac{\hbar^2}{2M}\left[\frac{d^2\psi_e(\rho)}{d\rho^2}-\frac{l^2}{\rho^2}\psi_e(\rho)\right]-E^e\psi_e(\rho)+\left(A\rho+\frac{1}{2}M\omega_{\text{b\_vib}}^2\rho^2\right)\psi_e(\rho)=0 \qquad \text{radial SE} \tag{S59}$$

and

$$-\frac{\hbar^2}{2M}\left[\frac{\partial^2\chi_e}{\partial\rho^2}+\frac{1}{\rho^2}\frac{\partial^2\chi_e}{\partial\phi^2}\right]-E^e\chi_e+\left(A\rho+\frac{1}{2}M\omega_{\text{b\_vib}}^2\rho^2\right)\chi_e=0, \qquad \text{total SE} \tag{S60}$$

where $\psi_e(\rho)=\rho^{1/2}u_e(\rho)$ and $\chi_e=\psi_e(\rho)e^{il\phi}$. Moreover, employing the equations of $\chi_\pm$, $\psi_e(\rho)$ and $u_e(\rho)$, χ_e can be expressed similarly in terms of $\chi_\pm$ as[5,6]:

$$\chi_e \;=\; \sqrt{\rho}\{\chi_+e^{i\phi/2}+\chi_-e^{-i\phi/2}\}. \tag{S61}$$

S2.2 Cubic perturbed pseudorotational levels in ground electronic state

Öpik and Pryce[4] introduced the higher order anharmonic term in the potential energy operator as:

$$V_-=A\begin{bmatrix}-Q_3 & -Q_2\\ -Q_2 & Q_3\end{bmatrix}+\frac{1}{2}M\omega_{\text{b\_vib}}^2\left(Q_2^2+Q_3^2\right)I+A_3Q_3\left(Q_3^2-3Q_2^2\right)I, \tag{S62}$$

where cubic term, $A_3Q_3\left(Q_3^2-3Q_2^2\right)$ transforms as $A_3\rho^3\cos 3\phi$ in the polar coordinate (ρ,ϕ) and the ground PES takes the following form:

$$V_-=-A\rho+\frac{1}{2}M\omega_{\text{b\_vib}}^2\rho^2+A_3\rho^3\cos 3\phi. \tag{S63}$$

Such anharmonic term of vibronic interaction leads to form regularly alternating hump/barrier and well/minimum in the 'Mexican Hat' APES.

The corresponding SE for cubic perturbed ground electronic state becomes:

$$-\frac{\hbar^2}{2M}\left[\frac{\partial^2}{\partial\rho^2}+\frac{1}{\rho^2}\frac{\partial^2}{\partial\phi^2}\right]\xi_g(\rho,\phi)-E\xi_g(\rho,\phi)$$
$$+\left(-A\rho+\frac{1}{2}M\omega^2_{\text{b\_vib}}\rho^2+A_3\rho^3\cos(3\phi)\right)\xi_g(\rho,\phi)=0. \tag{S64}$$

While investigating the motion of nuclei along the bottom of lower APES under the influence of such higher order electron-nuclear coupling term, O'Brien[7] averaged the above SE (Eq. (S64)) radially by restricting the radial part of perturbed wavefunction set ($\{\xi_g(\rho,\phi)[=w^0_g(\rho)\gamma(\phi)]\}$) to lowest harmonic vibrational eigenfunction ($w^0_g(\rho)$). As a result, the corresponding angular SE (Mathieu equation of C_{3v} symmetry group) turned into the following form:

$$\alpha\frac{\partial^2}{\partial\phi^2}\gamma(\phi)+\beta\cos(3\phi)\gamma(\phi)+\epsilon(\rho)\gamma(\phi)=0 \tag{S65}$$

and

$$\alpha=\langle w^0_g(\rho)|\frac{\hbar^2}{2M\rho^2}|w^0_g(\rho)\rangle$$
$$\beta=\langle w^0_g(\rho)|-A_3\rho^3|w^0_g(\rho)\rangle, \tag{S66}$$

where splitting, $\alpha(=\langle w^0_g(\rho)|\frac{\hbar^2}{2M\rho^2}|w^0_g(\rho)\rangle)$ and barrier, $\beta=(\langle w^0_g(\rho)|-A_3\rho^3|w^0_g(\rho)\rangle)$ parameters are approximated at the ground state minima (ρ_0) as $\alpha=\frac{\hbar^2}{2M\rho_0^2}$ and $\beta=-A_3\rho_0^3$, since the minima of lower sheet of APES are situated far away from the centre. In case of $[Cu(H_2O)_6]^{2+}$ complex, $\alpha=11$ cm^{-1} and $\beta\simeq 544$ cm^{-1}[6], whereas polarized Raman scattering[8,9] and structural phase transition study[10] of an untwinned $LaMnO_3$ single crystal provide the magnitude of α and β as 25 cm^{-1} and 375 cm^{-1}, respectively.

Expanding the angular wavefunction in Fourier series ($\gamma(\phi)=\sum_l a_l\exp(il\phi)$), the following recurrence relation of coefficients (a_l) is obtained from Eqs. S65 and S66:

$$a_l\left(\epsilon-\alpha l^2\right)+\frac{1}{2}\beta\left(a_{l-3}+a_{l+3}\right)=0. \tag{S67}$$

Secular determinant of such recursive relation, Eq. (S67) had been solved for a large spectrum of barrier parameter (β) values and the solutions, i.e., cubic perturbed pseudo - rotational energy profiles fall into the irreducible representations (IRREPs) of C_{3v} point group as[7](see Fig. S1): (i) $l = \pm\frac{3}{2}, \pm\frac{9}{2}, \pm\frac{15}{2}$, ... , is represented by A_1 for $a_l = +a_{-l}$, whereas it can be classified as A_2 if $a_l = -a_{-l}$; (ii) On the other hand, $l = +\frac{1}{2}, -\frac{5}{2}, +\frac{7}{2}, -\frac{11}{2}$, ..., and $l = -\frac{1}{2}, +\frac{5}{2}, -\frac{7}{2}, +\frac{11}{2}$, ... , transform as the two components of E, respectively. It is important to note that roto - vibrational levels, $l = \frac{3}{2}$ and $\frac{9}{2}$ undergo appreciable splitting due to the warping of lower branch of APES.

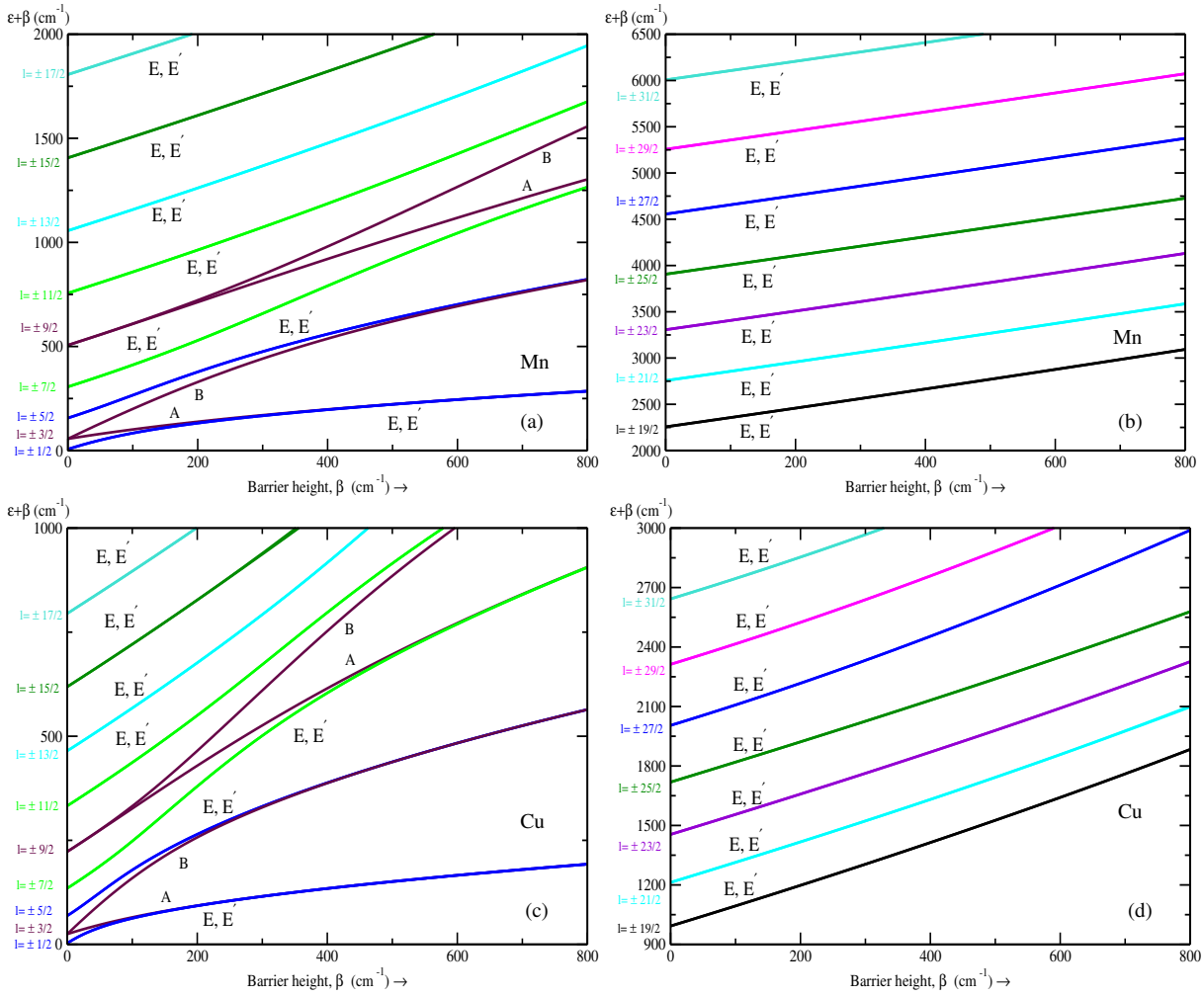

Fig. S1: The profiles of cubic perturbed roto-vibrational energy for different pseudo - rotational levels $l = \frac{1}{2}$, ...,$\frac{17}{2}$ and $l = \frac{19}{2}$, ..., $\frac{31}{2}$ with respect to barrier parameter β for $LaMnO_3$ (a)-(b) and $[Cu(H_2O)_6]^{2+}$ (c)-(d) complexes, respectively.

S2.3 Eigenvalues of Centrifugally Stabilized Excited State and Effect of Bond vibration

The frequencies of centrifugally stabilized excited oscillator depend on roto - vibrational quantum numbers ('l's) in a complicated manner unlike typical harmonic oscillator, which has particular one characteristic oscillation frequency; consequently, eigenspectrum of such centrifugally stabilized oscillator display unusual trend with the variation of pseudo - rotational quantum number (see Table S1).

Table S1: Eigenvalues for centrifugally stabilized excited state oscillators of various pseudo - rotational levels (l) without and with the inclusion of bond vibration (b_vib) for rare earth manganite, $LaMnO_3$ (the table is taken from Ref. [6]).

b_vib excluded	$l = \pm 1/2$	$l = \pm 3/2$	$l = \pm 5/2$	$l = \pm 7/2$	$l = \pm 9/2$	$l = \pm 11/2$	$l = \pm 13/2$	$l = \pm 15/2$
$E_{s=0,\,\pm l}$ [cm^{-1}]	2226.24	2976.35	3718.79	4404.46	5043.95	5646.74	6219.72	6767.88
$E_{s=1,\,\pm l}$ [cm^{-1}]	4612.31	4630.76	5114.17	5651.80	6191.05	6719.62	7234.49	7735.39
$E_{s=2,\,\pm l}$ [cm^{-1}]	6998.38	6285.17	6509.55	6899.14	7338.16	7792.51	8249.26	8702.89
b_vib included	$l = \pm 1/2$	$l = \pm 3/2$	$l = \pm 5/2$	$l = \pm 7/2$	$l = \pm 9/2$	$l = \pm 11/2$	$l = \pm 13/2$	$l = \pm 15/2$
$E^{b\_vib}_{s=0,\,\pm l}$ [cm$^-$1]	2252.05	3013.16	3762.06	4452.52	5095.87	5701.93	6277.75	6828.44
$E^{b\_vib}_{s=1,\,\pm l}$ [cm$^-$1]	4689.75	4741.19	5243.99	5795.98	6346.82	6885.19	7408.59	7917.06
$E^{b\_vib}_{s=2,\,\pm l}$ [cm$^-$1]	7127.45	6469.23	6725.93	7139.44	7597.77	8068.45	8539.42	9005.68

As a result of complex dependency on pseudo - rotational quantum numbers ('l's), energy levels $l = 1/2$ and $l = 3/2$ approach close to each other in the first excited state ($s = 1$), whereas in the second excited state, i.e., for $s = 2$, roto - vibrational level $l = 1/2$ goes above of $l = 7/2$ level in terms of the magnitude of energy[6,11] (see Table S1).

Furthermore, Table S1 also reflects that with the employment of bond vibration, eigenvalues of centrifugally stabilized vibronic levels are modified substantially such that roto - vibrational level $l = 1/2$ situates in between $l = \frac{5}{2}$ and $l = \frac{7}{2}$ level in second excited state ($s = 2$), which is contrary to without bond vibration case. It is very clear that entanglement with the bond vibration leads to the increase in overall energy of each pseudo - rotational level profoundly[6].

S2.4 Cubic Perturbed Centrifugally Stabilized Excited State: Bound States; Eigenvalues; Effect of Bond Vibration

On the contrary to the ground electronic state, cubic perturbed pseudo - rotational energies, ϵ_ls of various roto - vibrational levels form bound state with linear Jahn-Teller term, $A\rho$ in the excited state associated with the upper sheet of APES (see Fig. S2 (a)-(d)) due to the contribution of centrifugal term.

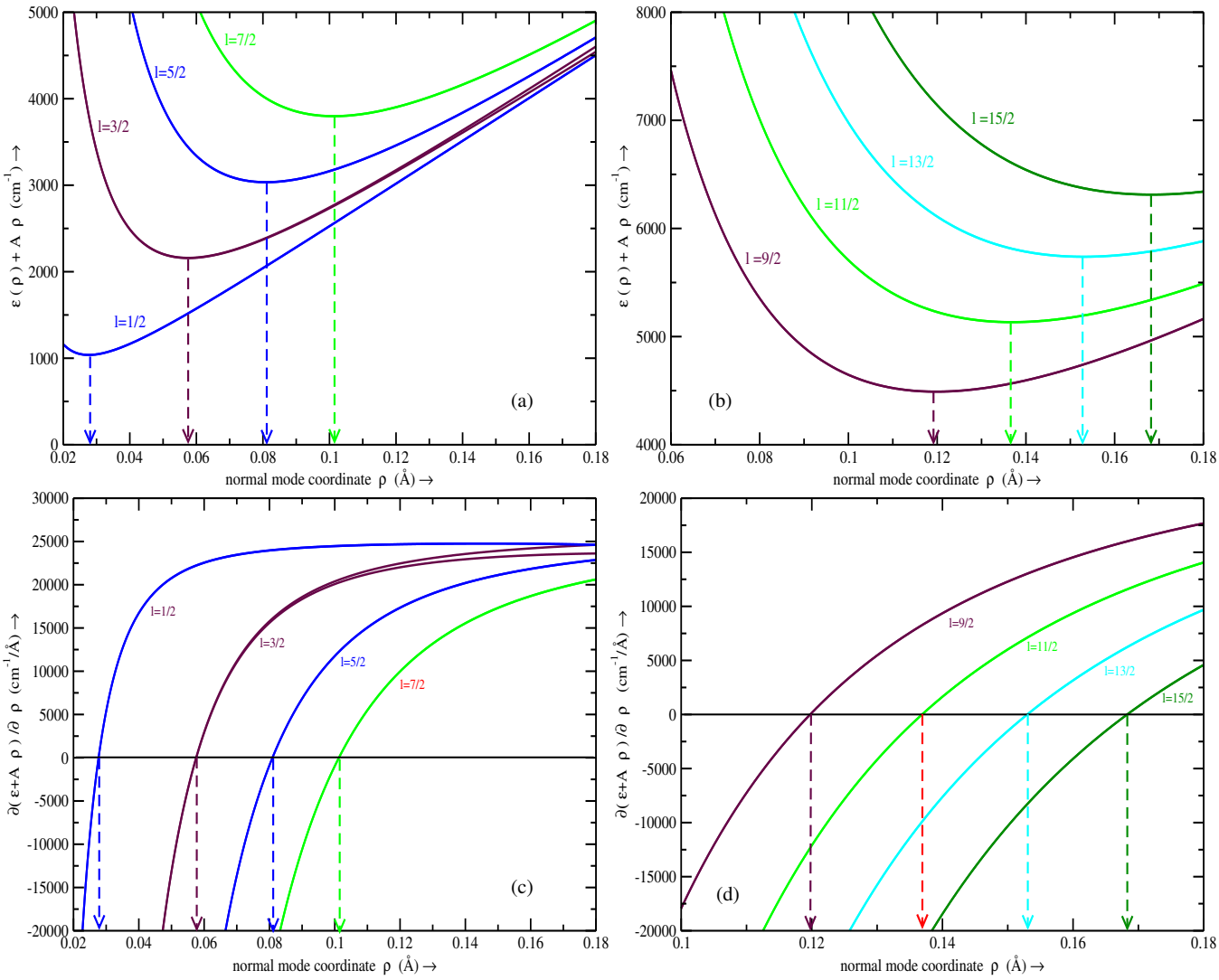

Fig. S2: Variation of effective potential $\epsilon_l(\rho) + A\rho$ as a function of ρ coordinate for different pseudorotational levels: (a) $l = \frac{1}{2}, \frac{3}{2}, \frac{5}{2}$, and $\frac{7}{2}$; (b) $l = \frac{9}{2}, \frac{11}{2}, \frac{13}{2}$, and $\frac{15}{2}$. Profiles of the derivatives of effective potential $\frac{\partial[\epsilon_l(\rho)+A\rho]}{\partial\rho}$ against ρ coordinate for various roto-vibrational levels: (c) $l = \frac{1}{2}, \frac{3}{2}, \frac{5}{2}$, and $\frac{7}{2}$; (d) $l = \frac{9}{2}, \frac{11}{2}, \frac{13}{2}$, and $\frac{15}{2}$ of cubic perturbed centrifugally stabilized excited state.

Table S2 depicts that under cubic perturbation, i.e., in presence of barrier (emerging from anhar-

monicity), roto-vibrational states $l = 3/2$, $l = 9/2$ and $l = 15/2$ undergo splitting. Furthermore, such magnitudes of splitting increase in the first ($s = 1$) and second ($s = 2$) excited states compare to ground one ($s = 0$) of centrifugally stabilized vibronic levels[6].

Table S2: Eigenvalues ($E^{cp}_{s,\pm l}$ [cm^{-1}]) for ground ($s = 0$), first ($s = 1$), and second ($s = 2$) excited states of cubic perturbed centrifugally stabilized oscillators of various roto-vibrational levels (l) (this table is taken from Ref. [6]).

Roto-vibrational level ($\pm l$)	$E^{cp}_{s=0,\pm l}$ (cm^{-1})	$E^{cp}_{s=1,\pm l}$ (cm^{-1})	$E^{cp}_{s=2,\pm l}$ (cm^{-1})
$\pm 1/2$	2228.22	4608.91	6989.61
	2228.22	4608.91	6989.61
$\pm 3/2$	2994.42	4657.10	6321.57
	2973.81	4611.32	6248.83
$\pm 5/2$	3731.39	5124.49	6517.59
	3731.39	5124.49	6517.59
$\pm 7/2$	4421.10	5667.11	6913.12
	4421.10	5667.11	6913.12
$\pm 9/2$	5064.69	6211.95	7359.21
	5064.35	6211.03	7357.70
$\pm 11/2$	5674.85	6753.95	7833.06
	5674.85	6753.95	7833.06
$\pm 13/2$	6255.12	7281.70	8308.27
	6255.12	7281.70	8308.27
$\pm 15/2$	6812.48	7799.28	8786.08
	6812.46	7799.22	8785.98

Moreover, Tables S2 and S3 reflect the fact that with the incorporation of harmonic bond vibration, every level experiences an increase in energy and the effect of energy order altering has been reduced both in first ($s = 1$) and second ($s = 2$) excited states of elastically entangled cubic perturbed centrifugally stabilized oscillators in comparison to the without bond vibration case[6].

Table S3: Cubic perturbed elastically (including bond vibration) coupled eigenvalues ($E^{cp\ +\ b\_vib}_{s,\ \pm l}$ [cm^{-1}]) for ground ($s = 0$), first ($s = 1$), and second ($s = 2$) excited states of cubic perturbed centrifugally stabilized oscillators of various pseudo - rotational levels (l) (the table is adapted from Ref. [6]).

Roto-vibrational level ($\pm l$)	$E^{cp\ +\ b\_vib}_{s=0,\ \pm l}$ [cm^{-1}]	$E^{cp\ +\ b\_vib}_{s=1,\ \pm l}$ [cm^{-1}]	$E^{cp\ +\ b\_vib}_{s=2,\ \pm l}$ [cm^{-1}]
±1/2	2254.09	4686.52	7118.96
	2254.09	4686.52	7118.96
±3/2	3031.03	4767.85	6504.66
	3010.98	4722.85	6434.71
±5/2	3774.73	5254.51	6734.30
	3774.73	5254.51	6734.30
±7/2	4469.21	5811.43	7153.66
	4469.21	5811.43	7153.66
±9/2	5116.61	6367.70	7618.79
	5116.30	6366.85	7617.40
±11/2	5729.75	6918.65	8107.60
	5729.75	6918.65	8107.60
±13/2	6312.56	7454.00	8595.44
	6312.56	7454.00	8595.44
±15/2	6871.98	7977.79	9083.59
	6871.96	7977.73	9083.50

S3 JT Condition for Model Octahedral Complex

In 1939, Van Vleck[12] carried out an extensive theoretical investigation on the JT distortion phenomenon of octahedrally coordinated complex, $M(H_2O)_6$ (M is a paramagnetic metal ion). Among the fifteen (15) normal modes, six (6) vibrations are classified as gerade (g) symmetric modes ($Q_1 \in a_{1g}$; $Q_2, Q_3 \in e_g$ and $Q_4, Q_5, Q_6 \in t_{2g}$) due to presence of center of symmetry (see Fig. S3). On the contrary, the center of symmetry is absent in rest of the normal mode coordinates and hence, those are designated as ungerade (u) symmetric modes. Since the symmetrized direct product of the degenerate electronic state (d orbitals) of the central metal atom $[\Gamma^{\alpha} \times \Gamma^{\alpha}]$ gives $\Gamma^{(g)}$ irreducible representation (IRREP), JT condition will be true only if $\Gamma^{\beta} = \Gamma^{(g)}$ [as $\Gamma^0 \in \Gamma^{\beta} \otimes [(\Gamma^{\alpha})^2]$, see Eq. 8 in the main article]. This implies that only the 'g' symmetric modes are responsible for JT

distortion in $M(H_2O)_6$ complex except the completely symmetric one (Q_1), which is unable to lift the degeneracy. Those six modes can be represented as the linear combinations of displacement vectors from the ideal octahedral arrangement (X_i, Y_i, Z_i),

$$
\begin{aligned}
Q_1 &= [X_1 - X_4 + Y_2 - Y_5 + Z_3 - Z_6]/\sqrt{6} \\
Q_2 &= \frac{1}{2}[X_1 - X_4 - Y_2 + Y_5] \\
Q_3 &= [\frac{1}{2}(X_1 - X_4 + Y_2 - Y_5) - Z_3 + Z_6]/\sqrt{3} \\
Q_4 &= \frac{1}{2}[Y_1 - Y_4 + X_2 - X_5] \\
Q_5 &= \frac{1}{2}[Z_1 - Z_4 + X_3 - X_6] \\
Q_6 &= \frac{1}{2}[Z_2 - Z_5 + Y_3 - Y_6]
\end{aligned}
$$

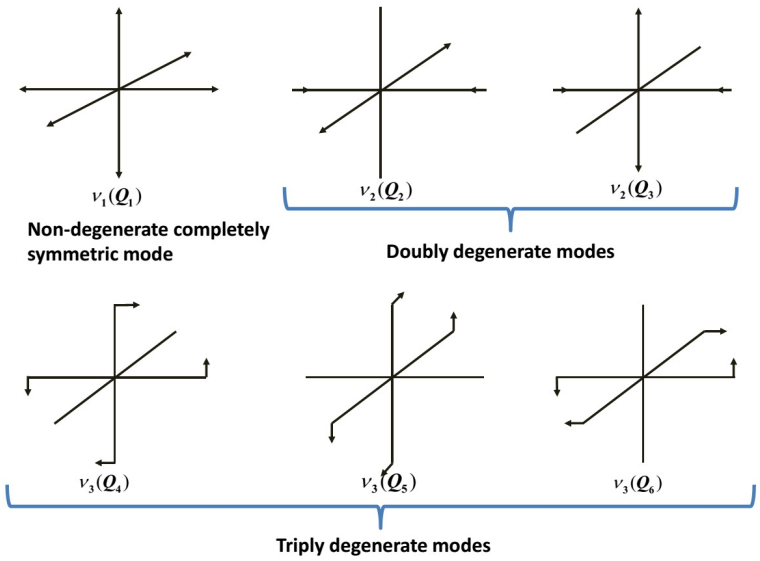

Fig. S3: The diagram depicts vectorial displacements of the bond lengths for six gerade (g) symmetric normal modes of the octahedrally coordinated complex ($M(H_2O)_6$).

It is important to mention that free $M(H_2O)_6$ complex belongs to octahedral point group (O_h), but in a crystal field environment, it exhibits a distortion along the axis of trigonal symmetry due to the external field originating from the bulk system.[12] Hence, it is more suitable to take a linear combination $\Big(Q'_4 = [\frac{1}{\sqrt{3}}(Q_4 + Q_5 + Q_6)]$, $Q'_5 = [\frac{1}{\sqrt{2}}(Q_5 - Q_6)]$, $Q'_6 = [\frac{1}{\sqrt{6}}(Q_5 + Q_6 - 2Q_4)]\Big)$ so that the distortion can be incorporated only along the Q'_4 mode keeping the remaining ones (Q'_5, Q'_6) unaltered.

In a crystal field environment, the Hamiltonian of $M(H_2O)_6$ complex takes the following form:

$$\begin{aligned}\hat{H} &= \hat{W}_0 + \hat{V}_{\text{trig}} \\ &+ \frac{1}{2}\alpha Q_1^2 + \frac{1}{2}\beta(Q_2^2 + Q_3^2) + \frac{1}{2}\gamma Q_4'^2 + \frac{1}{2}\delta(Q_5'^2 + Q_6'^2) \\ &+ V_2 Q_2 + V_3 Q_3 + V_4' Q_4' + V_5' Q_5' + V_6' Q_6' \end{aligned} \tag{S69}$$

In the above equation (Eq. S69), the unperturbed Hamiltonian for rotational and translational modes is collectively denoted by $\hat{W}_0$. On the other hand, $\hat{V}_{\text{trig}}$ signifies the potential experienced by the central metal atom due to the bulk crystal field. The quadratic functions of normal mode coordinates represent the unperturbed energy due to vibrational motions. Finally, the parameters, V_2 to V_3 and V_4' to V_6' represent the combining coefficients of linear perturbation, where the primed quantities obey similar relationship to the normal mode coordinates, i.e. $V_4' = \frac{1}{\sqrt{3}}(V_4 + V_5 + V_6)$, $V_5' = \frac{1}{\sqrt{2}}(V_5 - V_6)$ and $V_6' = \frac{1}{\sqrt{6}}(V_5 + V_6 - 2V_4)$. The coefficients, V_2 to V_6 are expressed as the summation over the contributions arising from the d electrons of metal atom,[12]

$$\begin{aligned} V_2 &= \sum_0 \{A(x_0^2 - y_0^2) + B(x_0^4 - y_0^4)\} + ... \\ V_3 &= \sum_0 \{A(x_0^2 + y_0^2 - 2z_0^2) + B(x_0^4 + y_0^4 - 2z_0^4)\}/\sqrt{3} + ... \\ V_4 &= \sum_0 \{Cx_0y_0 + E(x_0^3y_0 + x_0y_0^3)\} + ... \\ V_5 &= \sum_0 \{Cx_0z_0 + E(x_0^3z_0 + x_0z_0^3)\} + ... \\ V_6 &= \sum_0 \{Cy_0z_0 + E(y_0^3z_0 + y_0z_0^3)\} + ..., \end{aligned}$$

where $A = \frac{1}{4}ee_{EFF}(18R^{-4} - 75R^{-6}r_0^2)$, $B = 175ee_{EFF}/8R^6$, $C = ee_{EFF}(-6R^{-4} + 15R^{-6}r_0^2)$, $E = -35ee_{EFF}/2R^6$ and $r_0 = \sqrt{x_0^2 + y_0^2 + z_0^2}$. In the above expressions, e_{EFF} represents the field created by the corner atoms, e is the charge of the electron, R denotes the distance between the central atom (M) and one of the ligand (H_2O) in equilibrium, and $\{x_0, y_0, z_0\}$ symbolizes position coordinates of one d electron of M.

In summary, it needs to be mentioned that V_2 and V_3 belong to e_g (Γ^β) symmetry, whereas V_4' to V_6' can be assigned into t_{2g} (Γ^β) IRREP (similar to the IRREPs of normal mode coordinates). On the other hand, the symmetrized direct product $[\Gamma^\alpha \times \Gamma^\alpha]$ of doubly degenerate E (E_g/E_u) and triply degenerate T ($T_{1g}/T_{1u}/T_{2g}/T_{2u}$) states contain $A_{1g} + E_g$ and $A_{1g} + E_g + T_{2g}$ IRREPs,

respectively. Hence, according to JT condition [$\Gamma^0 \in \Gamma^\beta \otimes [(\Gamma^\alpha)^2]$, see Eq. 8 in the main article], V_2 and V_3 produce nonzero linear JT coupling ($\langle\phi_i^{(0)}|V_k|\phi_j^{(0)}\rangle$, $k = 2, 3$) for any E or T symmetric states, whereas V_4' to V_6' can lift the degeneracy of T symmetric ones only due to non-vanishing integrals ($\langle\phi_i^{(0)}|V_k'|\phi_j^{(0)}\rangle$, $k = 4 - 6$).

S4 Vibrational Modes of NO_3 and their Symmetry

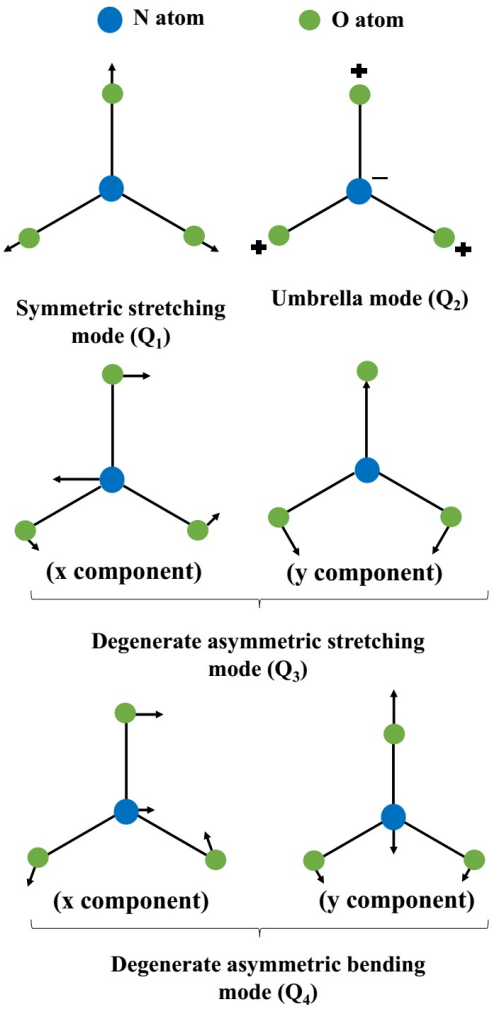

Fig. S4: The diagram depicts vectorial displacements of the bond lengths and bond angles for six normal modes of NO_3 radical. Displacements of the atoms in a plane is symbolized by the arrows, whereas, the $\pm$ sign indicates out of plane motion of those atoms.

Table S4: Character table of D_{3h} point group along with symmetry of the normal modes of NO_3

D_{3h}	E	$2C_3(z)$	$3C_2'$	$\sigma_h(xy)$	$2S_3$	$3\sigma_v$	linear functions, rotations	quadratic functions	normal modes of NO_3
A_1'	1	1	1	1	1	1		x^2+y^2,z^2	Q_1
A_2'	1	1	-1	1	1	-1	R_z		
E'	2	-1	0	2	-1	0	x, y	$(x^2-y^2$,$xy)$	$(Q_{3x}, Q_{3y}), (Q_{4x}, Q_{4y})$
A_1''	1	1	1	-1	-1	-1			
A_2''	1	1	-1	-1	-1	1	z		Q_2
E''	2	-1	0	-2	1	0	(R_x, R_y)	(xz, yz)	

S5 Adiabatic to Diabatic Transformation (ADT) Equations for three to five state Sub-Hilbert Space

S5.1 ADT equations for 3 state Sub-Hilbert space[13–15]

ADT matrix of three-state sub-Hilbert space for the combination $\mathbf{A}^{12}\mathbf{A}^{13}\mathbf{A}^{23}$ is given by:

$$\mathbf{A}(\Theta_{12}, \Theta_{13}, \Theta_{23}) = \mathbf{A}^{12}(\Theta_{12}) \cdot \mathbf{A}^{13}(\Theta_{13}) \cdot \mathbf{A}^{23}(\Theta_{23}),$$

$$= \begin{pmatrix} \cos\Theta_{12} & \sin\Theta_{12} & 0 \\ -\sin\Theta_{12} & \cos\Theta_{12} & 0 \\ 0 & 0 & 1 \end{pmatrix} \begin{pmatrix} \cos\Theta_{13} & 0 & \sin\Theta_{13} \\ 0 & 1 & 0 \\ -\sin\Theta_{13} & 0 & \cos\Theta_{13} \end{pmatrix} \begin{pmatrix} 1 & 0 & 0 \\ 0 & \cos\Theta_{23} & \sin\Theta_{23} \\ 0 & -\sin\Theta_{23} & \cos\Theta_{23} \end{pmatrix}$$

$$= \begin{pmatrix} \cos\Theta_{12}\cos\Theta_{13} & \sin\Theta_{12}\cos\Theta_{23} & \sin\Theta_{12}\sin\Theta_{23} \\ & -\cos\Theta_{12}\sin\Theta_{13}\sin\Theta_{23} & +\cos\Theta_{12}\sin\Theta_{13}\cos\Theta_{23} \\ -\sin\Theta_{12}\cos\Theta_{13} & \cos\Theta_{12}\cos\Theta_{23} & \cos\Theta_{12}\sin\Theta_{23} \\ & +\sin\Theta_{12}\sin\Theta_{13}\sin\Theta_{23} & -\sin\Theta_{12}\sin\Theta_{13}\cos\Theta_{23} \\ -\sin\Theta_{13} & -\cos\Theta_{13}\sin\Theta_{23} & \cos\Theta_{13}\cos\Theta_{23} \end{pmatrix},$$

where the ADT angles, Θ_{ij} are functions of nuclear coordinates. While using the ADT condition

as depicted in Eq. 32 of the main article, we obtain the following equations:

$$\begin{aligned}
\boldsymbol{\nabla}\Theta_{12} &= -\boldsymbol{\tau}^{12} - \tan\Theta_{13}(\boldsymbol{\tau}^{13}\sin\Theta_{12} + \boldsymbol{\tau}^{23}\cos\Theta_{12}),\\
\boldsymbol{\nabla}\Theta_{13} &= -(\boldsymbol{\tau}^{13}\cos\Theta_{12} - \boldsymbol{\tau}^{23}\sin\Theta_{12}),\\
\boldsymbol{\nabla}\Theta_{23} &= -\frac{1}{\cos\Theta_{13}}(\boldsymbol{\tau}^{13}\sin\Theta_{12} + \boldsymbol{\tau}^{23}\cos\Theta_{12}),
\end{aligned}$$

where $\boldsymbol{\tau}^{12}$, $\boldsymbol{\tau}^{13}$ and $\boldsymbol{\tau}^{23}$ are elements of nonadiabatic coupling matrix (NACM). For a three state electronic manifold with two nuclear degrees of freedom (for example, q and ϕ in Jacobi coordinates for F+H_2 system as depicted in Fig. S5), the components of NACM take the following form:

$$\tau_x(q,\phi) = \begin{pmatrix} 0 & \tau_x^{12}(q,\phi) & \tau_x^{13}(q,\phi) \\ -\tau_x^{12}(q,\phi) & 0 & \tau_x^{23}(q,\phi) \\ -\tau_x^{13}(q,\phi) & -\tau_x^{23}(q,\phi) & 0 \end{pmatrix}, \quad x = q \text{ or } \phi$$

and the two sets of scalar components of the ADT equations are as follows:

$$\begin{aligned}
\frac{\partial\Theta_{12}}{\partial q} &= -\tau_q^{12} - \tan\Theta_{13}(\tau_q^{13}\sin\Theta_{12} + \tau_q^{23}\cos\Theta_{12}), & \frac{\partial\Theta_{12}}{\partial\phi} &= -\tau_\phi^{12} - \tan\Theta_{13}(\tau_\phi^{13}\sin\Theta_{12} + \tau_\phi^{23}\cos\Theta_{12}),\\
\frac{\partial\Theta_{13}}{\partial q} &= -(\tau_q^{13}\cos\Theta_{12} - \tau_q^{23}\sin\Theta_{12}), & \frac{\partial\Theta_{13}}{\partial\phi} &= -(\tau_\phi^{13}\cos\Theta_{12} - \tau_\phi^{23}\sin\Theta_{12}),\\
\frac{\partial\Theta_{23}}{\partial q} &= -\frac{1}{\cos\Theta_{13}}(\tau_q^{13}\sin\Theta_{12} + \tau_q^{23}\cos\Theta_{12}). & \frac{\partial\Theta_{23}}{\partial\phi} &= -\frac{1}{\cos\Theta_{13}}(\tau_\phi^{13}\sin\Theta_{12} + \tau_\phi^{23}\cos\Theta_{12}).
\end{aligned}$$

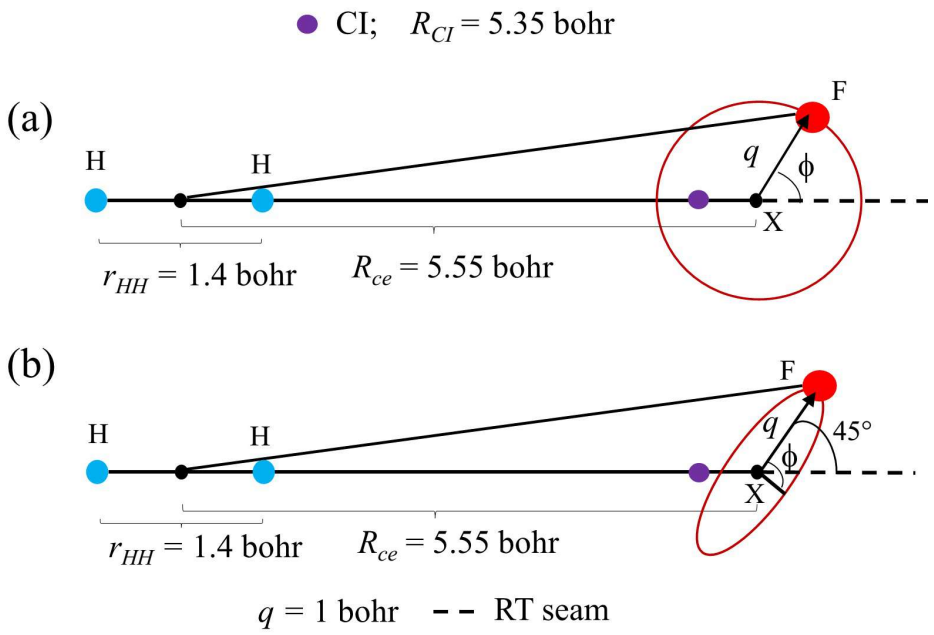

Fig. S5: In the above diagram, F is traversing along a closed contour of radius, $q = 1.0$ bohr around the center, X, where r_{HH} (H-H distance), R_{ce} (distance from the center of closed contour, X to the center of mass of H-H) and R_{CI} (distance from the conical intersection (CI) to the center of mass of H-H) are taken as 1.401 bohr, 5.55 bohr and 5.35 bohr, respectively. In both cases (a) and (b), the center of the circle is placed on the collinear H_2 axis. The circular path is (a) aligned in plane with the H-H-X axis to explore JT coupling and (b) tilted by 45° with respect to the same axis to calculate the Renner-Teller (RT) interactions present in this triatomic reactive system.

S5.2 ADT equations for 4 state Sub-Hilbert space[16]

We present the ADT equations for a set of four (4) coupled electronic states considering the following order of multiplication of the elementary rotation matrices:

$$\mathbf{A}(\Theta_{12},\Theta_{13},\Theta_{23},\Theta_{14},\Theta_{24},\Theta_{34}) = \mathbf{A}^{12}(\Theta_{12})\cdot\mathbf{A}^{13}(\Theta_{13})\cdot\mathbf{A}^{23}(\Theta_{23})\cdot\mathbf{A}^{14}(\Theta_{14})\cdot\mathbf{A}^{24}(\Theta_{24})\cdot\mathbf{A}^{34}(\Theta_{34})$$

Employing the ADT condition (Eq. 32 in the main article), such equations are formulated as,

$$\begin{aligned}
\boldsymbol{\nabla}\Theta_{12} &= -\boldsymbol{\tau}^{12} - \sin\Theta_{12}(\boldsymbol{\tau}^{13}\tan\Theta_{13} + \boldsymbol{\tau}^{14}\sec\Theta_{13}\tan\Theta_{14}) \\
&\quad - \cos\Theta_{12}(\boldsymbol{\tau}^{23}\tan\Theta_{13} + \boldsymbol{\tau}^{24}\sec\Theta_{13}\tan\Theta_{14}) \\
\\
\boldsymbol{\nabla}\Theta_{13} &= -\boldsymbol{\tau}^{34}\cos\Theta_{13}\tan\Theta_{14} + \sin\Theta_{12}(\boldsymbol{\tau}^{23} + \boldsymbol{\tau}^{24}\sin\Theta_{13}\tan\Theta_{14}) - \\
&\quad \cos\Theta_{12}(\boldsymbol{\tau}^{13} + \boldsymbol{\tau}^{14}\sin\Theta_{13}\tan\Theta_{14}) \\
\\
\boldsymbol{\nabla}\Theta_{14} &= -\boldsymbol{\tau}^{14}\cos\Theta_{12}\cos\Theta_{13} + \boldsymbol{\tau}^{24}\sin\Theta_{12}\cos\Theta_{13} + \boldsymbol{\tau}^{34}\sin\Theta_{13} \\
\\
\boldsymbol{\nabla}\Theta_{23} &= -\cos\Theta_{13}[\boldsymbol{\tau}^{13}\sin\Theta_{12}\sec^2\Theta_{13} \\
&\quad +(\boldsymbol{\tau}^{34} - \boldsymbol{\tau}^{24}\sin\Theta_{12}\tan\Theta_{13})\cos\Theta_{23}\sec\Theta_{14}\tan\Theta_{24} \\
&\quad +\boldsymbol{\tau}^{14}\sin\Theta_{12}\sec\Theta_{13}(\tan\Theta_{13}\tan\Theta_{14} + \sin\Theta_{23}\sec\Theta_{14}\tan\Theta_{24}) \\
&\quad +\cos\Theta_{12}\{\boldsymbol{\tau}^{23}\sec^2\Theta_{13} + \boldsymbol{\tau}^{14}\tan\Theta_{13}\cos\Theta_{23}\sec\Theta_{14}\tan\Theta_{24} \\
&\quad +\boldsymbol{\tau}^{24}(\sec\Theta_{13}\tan\Theta_{13}\tan\Theta_{14} + \sin\Theta_{23}\sec\Theta_{14}\tan\Theta_{24})\}] \\
\\
\boldsymbol{\nabla}\Theta_{24} &= -\boldsymbol{\tau}^{24}\sin\Theta_{12}\sin\Theta_{13}\sec\Theta_{14}\sin\Theta_{23} + \boldsymbol{\tau}^{34}\cos\Theta_{13}\sec\Theta_{14}\sin\Theta_{23} \\
&\quad -\boldsymbol{\tau}^{14}(\sin\Theta_{12}\cos\Theta_{23}\sec\Theta_{14} - \cos\Theta_{12}\sin\Theta_{13}\sec\Theta_{14}\sin\Theta_{23}) \\
&\quad -\boldsymbol{\tau}^{24}\cos\Theta_{12}\cos\Theta_{23}\sec\Theta_{14} \\
\\
\boldsymbol{\nabla}\Theta_{34} &= -\boldsymbol{\tau}^{14}\sin\Theta_{12}\sin\Theta_{23}\sec\Theta_{14}\sec\Theta_{24} + \boldsymbol{\tau}^{24}\sin\Theta_{12}\sin\Theta_{13}\cos\Theta_{23}\sec\Theta_{14}\sec\Theta_{24} \\
&\quad -\boldsymbol{\tau}^{14}\cos\Theta_{12}\sec\Theta_{24}\sin\Theta_{13}\cos\Theta_{23}\sec\Theta_{14} - \boldsymbol{\tau}^{24}\cos\Theta_{12}\sin\Theta_{23}\sec\Theta_{14}\sec\Theta_{24} \\
&\quad -\boldsymbol{\tau}^{34}\cos\Theta_{13}\cos\Theta_{23}\sec\Theta_{14}\sec\Theta_{24}
\end{aligned}$$

S5.3 ADT equations for 5 state Sub-Hilbert space[17]

In case of five (5) coupled electronic states, the ADT matrix is constructed by taking the product of ten (10) rotation matrices according to the following order:

$$\mathbf{A} = \mathbf{A}^{12}(\Theta_{12}).\mathbf{A}^{13}(\Theta_{13}).\mathbf{A}^{23}(\Theta_{23}).\mathbf{A}^{14}(\Theta_{14}).\mathbf{A}^{24}(\Theta_{24}).\mathbf{A}^{34}(\Theta_{34}).\mathbf{A}^{15}(\Theta_{15}).\mathbf{A}^{25}(\Theta_{25}).\mathbf{A}^{35}(\Theta_{35}).\mathbf{A}^{45}(\Theta_{45})$$

The ADT equations are,

$$\begin{aligned}
\boldsymbol{\nabla}\Theta_{12} &= -\boldsymbol{\tau}^{12} - \sin\Theta_{12}(\boldsymbol{\tau}^{13}\tan\Theta_{13} + \boldsymbol{\tau}^{14}\sec\Theta_{13}\tan\Theta_{14} + \boldsymbol{\tau}^{15}\sec\Theta_{13}\sec\Theta_{14}\tan\Theta_{15}) - \cos\Theta_{12}\{\boldsymbol{\tau}^{23}\tan\Theta_{13} \\
&\quad + \sec\Theta_{13}(\boldsymbol{\tau}^{24}\tan\Theta_{14} + \boldsymbol{\tau}^{25}\sec\Theta_{14}\tan\Theta_{15})\}
\end{aligned}$$

$$\begin{aligned}
\boldsymbol{\nabla}\Theta_{13} &= -\cos\Theta_{13}(\boldsymbol{\tau}^{34}\tan\Theta_{14} + \boldsymbol{\tau}^{35}\sec\Theta_{14}\tan\Theta_{15}) + \sin\Theta_{12}(\boldsymbol{\tau}^{23} + \boldsymbol{\tau}^{24}\sin\Theta_{13}\tan\Theta_{14} + \boldsymbol{\tau}^{25}\sin\Theta_{13}\sec\Theta_{14} \\
&\quad \tan\Theta_{15}) - \cos\Theta_{12}\{\boldsymbol{\tau}^{13} + \sin\Theta_{13}(\boldsymbol{\tau}^{14}\tan\Theta_{14} + \boldsymbol{\tau}^{15}\sec\Theta_{14}\tan\Theta_{15})\}
\end{aligned}$$

$$\begin{aligned}
\boldsymbol{\nabla}\Theta_{23} &= -\cos\Theta_{13}[\boldsymbol{\tau}^{13}\sin\Theta_{12}\sec^2\Theta_{13} + \cos\Theta_{23}\{\sec\Theta_{14}(\boldsymbol{\tau}^{34} - \boldsymbol{\tau}^{24}\sin\Theta_{12}\tan\Theta_{13})\tan\Theta_{24} + (\boldsymbol{\tau}^{35} \\
&\quad -\boldsymbol{\tau}^{25}\sin\Theta_{12}\tan\Theta_{13})(\tan\Theta_{14}\tan\Theta_{15}\tan\Theta_{24} + \sec\Theta_{15}\sec\Theta_{24}\tan\Theta_{25})\} + \sin\Theta_{12}\sec\Theta_{13}\{\tan\Theta_{13} \\
&\quad (\boldsymbol{\tau}^{14}\tan\Theta_{14} + \boldsymbol{\tau}^{15}\sec\Theta_{14}\tan\Theta_{15}) + \sin\Theta_{23}(\boldsymbol{\tau}^{14}\sec\Theta_{14}\tan\Theta_{24} + \boldsymbol{\tau}^{15}\tan\Theta_{14}\tan\Theta_{15}\tan\Theta_{24} \\
&\quad +\boldsymbol{\tau}^{15}\sec\Theta_{15}\sec\Theta_{24}\tan\Theta_{25})\} + \cos\Theta_{12}\{\boldsymbol{\tau}^{23}\sec^2\Theta_{13} + \tan\Theta_{13}\cos\Theta_{23}(\boldsymbol{\tau}^{14}\sec\Theta_{14}\tan\Theta_{24} \\
&\quad +\boldsymbol{\tau}^{15}\tan\Theta_{14}\tan\Theta_{15}\tan\Theta_{24} + \boldsymbol{\tau}^{15}\sec\Theta_{15}\sec\Theta_{24}\tan\Theta_{25}) + \sec\Theta_{13}(\tan\Theta_{13}(\boldsymbol{\tau}^{24}\tan\Theta_{14} \\
&\quad +\boldsymbol{\tau}^{25}\sec\Theta_{14}\tan\Theta_{15}) + \sin\Theta_{23}(\boldsymbol{\tau}^{24}\sec\Theta_{14}\tan\Theta_{24} + \boldsymbol{\tau}^{25}\tan\Theta_{14}\tan\Theta_{15}\tan\Theta_{24} \\
&\quad +\boldsymbol{\tau}^{25}\sec\Theta_{15}\sec\Theta_{24}\tan\Theta_{25}))\}]
\end{aligned}$$

$$\begin{aligned}
\boldsymbol{\nabla}\Theta_{14} &= -\boldsymbol{\tau}^{45}\cos\Theta_{14}\tan\Theta_{15} - \cos\Theta_{12}\cos\Theta_{13}(\boldsymbol{\tau}^{14} + \boldsymbol{\tau}^{15}\sin\Theta_{14}\tan\Theta_{15}) + \sin\Theta_{12}\cos\Theta_{13}(\boldsymbol{\tau}^{24} + \boldsymbol{\tau}^{25}\sin\Theta_{14} \\
&\quad \tan\Theta_{15}) + \sin\Theta_{13}(\boldsymbol{\tau}^{34} + \boldsymbol{\tau}^{35}\sin\Theta_{14}\tan\Theta_{15})
\end{aligned}$$

$$
\begin{aligned}
\boldsymbol{\nabla}\Theta_{24} &= \sin\Theta_{23}\{-\sin\Theta_{12}\sin\Theta_{13}(\boldsymbol{\tau}^{24}\sec\Theta_{14}+\boldsymbol{\tau}^{25}\tan\Theta_{14}\tan\Theta_{15})+\cos\Theta_{13}(\boldsymbol{\tau}^{34}\sec\Theta_{14}\\
&\quad+\boldsymbol{\tau}^{35}\tan\Theta_{14}\tan\Theta_{15})\}+\sec\Theta_{15}\{-\boldsymbol{\tau}^{45}\cos\Theta_{14}\cos\Theta_{24}+\cos\Theta_{24}(\boldsymbol{\tau}^{25}\cos\Theta_{13}\sin\Theta_{14}\\
&\quad+\boldsymbol{\tau}^{35}\sin\Theta_{13})\sin\Theta_{14}+(\boldsymbol{\tau}^{35}\cos\Theta_{13}-\boldsymbol{\tau}^{25}\sin\Theta_{12}\sin\Theta_{13})\sin\Theta_{23}\sin\Theta_{24}\}\tan\Theta_{25}\\
&\quad-\sin\Theta_{12}\cos\Theta_{23}(\boldsymbol{\tau}^{14}\sec\Theta_{14}+\boldsymbol{\tau}^{15}\tan\Theta_{14}\tan\Theta_{15}+\boldsymbol{\tau}^{15}\sec\Theta_{15}\sin\Theta_{24}\tan\Theta_{25})\\
&\quad+\cos\Theta_{12}\{\sin\Theta_{13}\sin\Theta_{23}(\boldsymbol{\tau}^{14}\sec\Theta_{14}+\boldsymbol{\tau}^{15}\tan\Theta_{14}\tan\Theta_{15})\\
&\quad+\boldsymbol{\tau}^{15}\sec\Theta_{15}(-\cos\Theta_{13}\cos\Theta_{24}\sin\Theta_{14}+\sin\Theta_{13}\sin\Theta_{23}\sin\Theta_{24})\tan\Theta_{25}\\
&\quad-\cos\Theta_{23}(\boldsymbol{\tau}^{24}\sec\Theta_{14}+\boldsymbol{\tau}^{25}\tan\Theta_{14}\tan\Theta_{15}+\boldsymbol{\tau}^{25}\sec\Theta_{15}\sin\Theta_{24}\tan\Theta_{25})\}
\end{aligned}
$$

$$
\begin{aligned}
\boldsymbol{\nabla}\Theta_{34} &= \sin\Theta_{12}\{-\sin\Theta_{23}(\boldsymbol{\tau}^{14}\sec\Theta_{14}\sec\Theta_{24}+\boldsymbol{\tau}^{15}\tan\Theta_{14}\tan\Theta_{15}\sec\Theta_{24}+\boldsymbol{\tau}^{15}\sec\Theta_{15}\tan\Theta_{24}\tan\Theta_{25})\\
&\quad+\sin\Theta_{13}\cos\Theta_{23}(\boldsymbol{\tau}^{24}\sec\Theta_{14}\sec\Theta_{24}+\boldsymbol{\tau}^{25}\tan\Theta_{14}\tan\Theta_{15}\sec\Theta_{24}+\boldsymbol{\tau}^{25}\sec\Theta_{15}\tan\Theta_{24}\tan\Theta_{25})\}\\
&\quad-\sec\Theta_{15}\sec\Theta_{25}[\cos\Theta_{34}\{\boldsymbol{\tau}^{45}\cos\Theta_{14}\cos\Theta_{24}-\boldsymbol{\tau}^{35}\sin\Theta_{13}\sin\Theta_{14}\cos\Theta_{24}+\sin\Theta_{12}(\boldsymbol{\tau}^{15}\cos\Theta_{23}\\
&\quad+\boldsymbol{\tau}^{25}\sin\Theta_{13}\sin\Theta_{23})\sin\Theta_{24}\}+\sin\Theta_{12}(-\boldsymbol{\tau}^{25}\sin\Theta_{13}\cos\Theta_{23}+\boldsymbol{\tau}^{15}\sin\Theta_{23})\sin\Theta_{34}]\tan\Theta_{35}+\cos\Theta_{12}\\
&\quad[-\sec\Theta_{24}\{\sin\Theta_{13}\cos\Theta_{23}(\boldsymbol{\tau}^{14}\sec\Theta_{14}+\boldsymbol{\tau}^{15}\tan\Theta_{14}\tan\Theta_{15})+\sin\Theta_{23}(\boldsymbol{\tau}^{24}\sec\Theta_{14}+\boldsymbol{\tau}^{25}\tan\Theta_{14}\\
&\quad\tan\Theta_{15})\}-\sec\Theta_{15}(\boldsymbol{\tau}^{15}\sin\Theta_{13}\cos\Theta_{23}+\boldsymbol{\tau}^{25}\sin\Theta_{23})\tan\Theta_{24}\tan\Theta_{25}-\sec\Theta_{15}\sec\Theta_{25}\{\cos\Theta_{34}\\
&\quad(\boldsymbol{\tau}^{25}\cos\Theta_{23}-\boldsymbol{\tau}^{15}\sin\Theta_{13}\sin\Theta_{23})\sin\Theta_{24}+(\boldsymbol{\tau}^{15}\sin\Theta_{13}\cos\Theta_{23}+\boldsymbol{\tau}^{25}\sin\Theta_{23})\sin\Theta_{34}\}\tan\Theta_{35}]\\
&\quad+\cos\Theta_{13}[\sec\Theta_{15}\sec\Theta_{25}\cos\Theta_{34}\{\cos\Theta_{24}(-\boldsymbol{\tau}^{15}\cos\Theta_{12}+\boldsymbol{\tau}^{25}\sin\Theta_{12})\sin\Theta_{14}+\boldsymbol{\tau}^{35}\sin\Theta_{23}\sin\Theta_{24}\}\\
&\quad\tan\Theta_{35}-\cos\Theta_{23}(\boldsymbol{\tau}^{34}\sec\Theta_{14}\sec\Theta_{24}+\boldsymbol{\tau}^{35}\tan\Theta_{14}\tan\Theta_{15}\sec\Theta_{24}+\boldsymbol{\tau}^{35}\sec\Theta_{15}\tan\Theta_{24}\tan\Theta_{25}\\
&\quad+\boldsymbol{\tau}^{35}\sec\Theta_{15}\sec\Theta_{25}\sin\Theta_{34}\tan\Theta_{35})]
\end{aligned}
$$

$$
\boldsymbol{\nabla}\Theta_{15} = -\boldsymbol{\tau}^{15}\cos\Theta_{12}\cos\Theta_{13}\cos\Theta_{14}+\boldsymbol{\tau}^{25}\sin\Theta_{12}\cos\Theta_{13}\cos\Theta_{14}+\boldsymbol{\tau}^{35}\sin\Theta_{13}\cos\Theta_{14}+\boldsymbol{\tau}^{45}\sin\Theta_{14}
$$

$$
\begin{aligned}
\boldsymbol{\nabla}\Theta_{25} &= \sec\Theta_{15}[\cos\Theta_{24}\{-\cos\Theta_{23}(\boldsymbol{\tau}^{25}\cos\Theta_{12}+\boldsymbol{\tau}^{15}\sin\Theta_{12})+(\boldsymbol{\tau}^{35}\cos\Theta_{13}\\
&\quad+(\boldsymbol{\tau}^{15}\cos\Theta_{12}-\boldsymbol{\tau}^{25}\sin\Theta_{12})\sin\Theta_{13})\sin\Theta_{23}\}+\{\boldsymbol{\tau}^{45}\cos\Theta_{14}+(\boldsymbol{\tau}^{15}\cos\Theta_{12}\cos\Theta_{13}\\
&\quad-\boldsymbol{\tau}^{25}\sin\Theta_{12}\cos\Theta_{13}-\boldsymbol{\tau}^{35}\sin\Theta_{13})\sin\Theta_{14}\}\sin\Theta_{24}]
\end{aligned}
$$

$$
\begin{aligned}
\boldsymbol{\nabla}\Theta_{35} &= \sec\Theta_{15}\sec\Theta_{25}[-\cos\Theta_{34}\{\boldsymbol{\tau}^{35}\cos\Theta_{13}\cos\Theta_{23}+\cos\Theta_{23}(\boldsymbol{\tau}^{15}\cos\Theta_{12}-\boldsymbol{\tau}^{25}\sin\Theta_{12})\sin\Theta_{13}+(\boldsymbol{\tau}^{25}\cos\Theta_{12}\\
&\quad+\boldsymbol{\tau}^{15}\sin\Theta_{12})\sin\Theta_{23}\}+\{\boldsymbol{\tau}^{45}\cos\Theta_{14}\cos\Theta_{24}+\cos\Theta_{24}(\boldsymbol{\tau}^{15}\cos\Theta_{12}\cos\Theta_{13}-\boldsymbol{\tau}^{25}\sin\Theta_{12}\cos\Theta_{13}\\
&\quad-\boldsymbol{\tau}^{35}\sin\Theta_{13})\sin\Theta_{14}+(\cos\Theta_{23}(\boldsymbol{\tau}^{25}\cos\Theta_{12}+\boldsymbol{\tau}^{15}\sin\Theta_{12})-(\boldsymbol{\tau}^{35}\cos\Theta_{13}+(\boldsymbol{\tau}^{15}\cos\Theta_{12}\\
&\quad-\boldsymbol{\tau}^{25}\sin\Theta_{12})\sin\Theta_{13})\sin\Theta_{23})\sin\Theta_{24}\}\sin\Theta_{34}]
\end{aligned}
$$

$$
\begin{aligned}
\boldsymbol{\nabla}\Theta_{45} &= \sec\Theta_{15}\sec\Theta_{25}\sec\Theta_{35}[\cos\Theta_{34}\{-\boldsymbol{\tau}^{45}\cos\Theta_{14}\cos\Theta_{24}+\cos\Theta_{24}(-\boldsymbol{\tau}^{15}\cos\Theta_{12}\cos\Theta_{13}\\
&\quad+\boldsymbol{\tau}^{25}\sin\Theta_{12}\cos\Theta_{13}+\boldsymbol{\tau}^{35}\sin\Theta_{13})\sin\Theta_{14}-(\cos\Theta_{23}(\boldsymbol{\tau}^{25}\cos\Theta_{12}+\boldsymbol{\tau}^{15}\sin\Theta_{12})-\\
&\quad(\boldsymbol{\tau}^{35}\cos\Theta_{13}+(\boldsymbol{\tau}^{15}\cos\Theta_{12}-\boldsymbol{\tau}^{25}\sin\Theta_{12})\sin\Theta_{13})\sin\Theta_{23})\sin\Theta_{24}\}-\\
&\quad\{\boldsymbol{\tau}^{35}\cos\Theta_{13}\cos\Theta_{23}+\cos\Theta_{23}(\boldsymbol{\tau}^{15}\cos\Theta_{12}-\boldsymbol{\tau}^{25}\sin\Theta_{12})\sin\Theta_{13}\\
&\quad+(\boldsymbol{\tau}^{25}\cos\Theta_{12}+\boldsymbol{\tau}^{15}\sin\Theta_{12})\sin\Theta_{23}\}\sin\Theta_{34}]
\end{aligned}
$$

S6 Molecular Symmetry Adaptation for D_{3h} System

Theorem 1: If the IRREP of a nonadiabatic coupling term (NACT), τ_l^{ij} is known along a specific symmetry adapted nuclear degree of freedom (DOF), R_l, the IRREP of the another one, τ_k^{ij} along a different symmetry adapted nuclear coordinate, R_k can be obtained by implementing the following relationship:[18]

$$\Gamma(\tau_k^{ij}) \quad = \quad \Gamma\left(\frac{\partial}{\partial R_k}\right) \times \Gamma\left(\frac{\partial}{\partial R_l}\right) \times \Gamma(\tau_l^{ij}), \tag{S74}$$

where

$$\tau_k^{ij} \quad = \quad \left\langle \xi_i \middle| \frac{\partial \xi_j}{\partial R_k} \right\rangle. \tag{S75}$$

Employing the above criterion, one can determine the possible combinations of the IRREPs by fixing each of the NACTs [τ_ks ($k = \rho$ and ϕ or x and y)] to the totally symmetric one (A_1'), successively. For D_{3h}(M) Molecular Symmetry (MS) group, if we choose $\tau_\rho \in A_1'$, it can be found from Table S5 and Eq. S74 that $\tau_\phi \in A_1''$ and τ_x, $\tau_y \in E''$. Similarly, if the IRREP of τ_ϕ is assumed as A_1', we obtain $\tau_\rho \in A_1''$ and τ_x, $\tau_y \in E'$. On the contrary, for other two possibilities ($\tau_x \in A_1'$ or $\tau_y \in A_1'$), τ_y or τ_x belongs to *reducible representation*, which contradicts the construction of Character Table[19] as depicted in Table S5.

Table S5: Extended character table of molecular symmetry group $D_{3h}(M)$ with different components of NACT. This table is adapted from Ref. [15].

D_{3h}(M)	E	(123) (132)	(12) (13) (23)	$E^\star$	(123)* (132)*	(12)* (13)* (23)*	coord.	deriv.	1st comb.	2nd comb.
A_1'	1	1	1	1	1	1			τ_ρ	τ_ϕ
A_2'	1	1	-1	1	1	-1	ϕ	$\frac{\partial}{\partial \phi}$		
E'	2	-1	0	2	-1	0	x, y	$\frac{\partial}{\partial x}$, $\frac{\partial}{\partial y}$		τ_x, τ_y
A_1''	1	1	1	-1	-1	-1			τ_ϕ	τ_ρ
A_2''	1	1	-1	-1	-1	1	ρ	$\frac{\partial}{\partial \rho}$		
E''	2	-1	0	-2	1	0			τ_x,τ_y	

Among the two possible combinations depicted above, the second one ($\tau_\phi \in A_1'$, $\tau_\rho \in A_1''$ and τ_x, $\tau_y \in E'$) is compatible to the quantization rule, which is demonstrated in the following para-

graphs.

Fig. S6 depicts the nodal patterns of the NACTs[19,20] for all possible IRREPs, which are presented as functions of normal mode coordinates, Q_x (bending) and Q_y (asymmetric stretching) of Na_3 cluster. In this diagram, the inner and outer concentric circles signify $Q_x - Q_y$ plane for positive and negative values of Q_s (symmetric stretching), respectively. In order to find the correct combination of IRREPs from the two possible ones (see Table S5), we consider the smaller circles of Fig. S6 and apply the following quantization rule[21] along a closed path L_g of nuclear coordinate $\mathbf{R}$ around a single CI:

$$\oint d\mathbf{R} \cdot \boldsymbol{\tau}(\mathbf{R}; L_g) \quad = \quad \pm\pi \tag{S76}$$

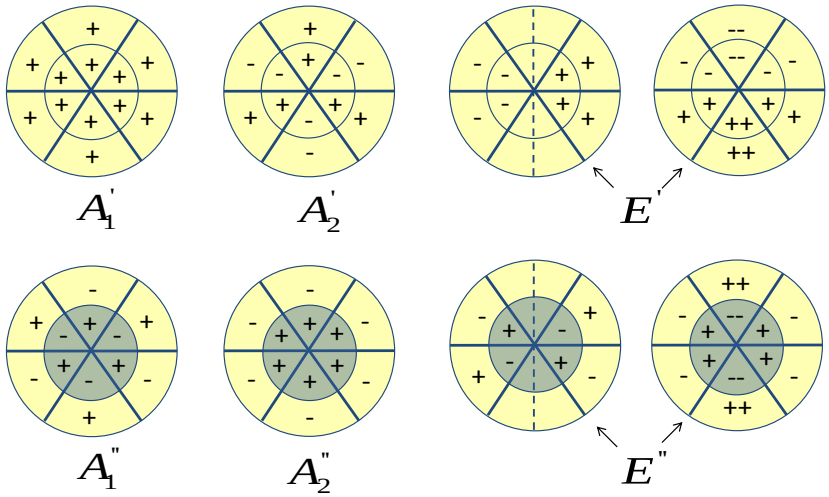

Fig. S6: Nodal patterns of IRREPs of D_{3h} point group. This figure is adapted from Ref. [15].

According to Fig. S7, this closed contour can be constructed by three components,[18] namely, one torsional (tor) and two radial (rad) lines and then, the contour integral takes the following form:

$$\oint d\mathbf{R} \cdot \boldsymbol{\tau}(\mathbf{R}; L_g) \quad = \quad I_{\text{rad},1} + I_{\text{tor}} + I_{\text{rad},2} = \pm\pi,$$

where

$$I_{\text{rad},1} = \int_0^{\rho_1} d\rho \; \tau_\rho(\rho, \phi_1; L_g), \; I_{\text{tor}} = \int_{\phi_1}^{\phi_2} d\phi \; \tau_\phi(\rho_1, \phi; L_g)$$

$$\text{and} \qquad I_{\text{rad},2} = \int_{\rho_1}^{0} d\rho \; \tau_\rho(\rho, \phi_2; L_g).$$

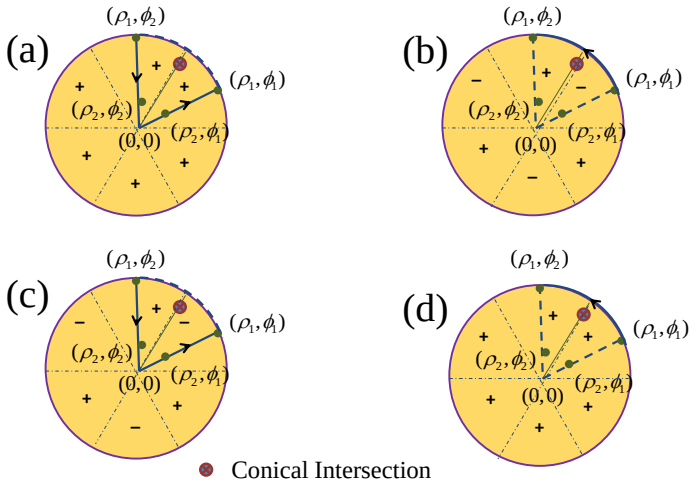

Fig. S7: For 1st combination of IRREPs of the NACTs, the radial and torsional parts of a closed loop L_g encircling a CI point in (ρ, ϕ) plane are depicted in diagrams (a) and (b). On the other hand, the same quantities for the 2nd combination are demonstrated in diagrams (c) and (d). Figures are taken from Ref. [15].

Fig. S7 (a-b) depict $I_{rad,1} + I_{rad,2} = 0$ and $I_{tor} = 0$ for the first combination ($\tau_\rho \in A_1'$, $\tau_\phi \in A_1''$, τ_x, $\tau_y \in E''$). On the contrary, the second combination ($\tau_\phi \in A_1'$, $\tau_\rho \in A_1''$ and τ_x, $\tau_y \in E'$) produces non-zero residue for the contour integral [see Fig. S7 (c-d)]. Therefore, it is worthwhile to mention that only the second set of IRREPs is the physically meaningful one.

Theorem 2: For a specific nuclear DOF (l), if the IRREP of a particular NACT within two electronic states (p and q), τ_l^{pq} is either known or assumed, it is possible to find out the IRREP of another one (τ_l^{qr}) within two electronic states, q and r.

For a loop-type sequence of N molecular states with same spin multiplicity, namely, N doublet states of Na_3 cluster, D_a, D_b, D_c,....., D_y, $D_{z=a}$, the product of the NACTs ($\tau_k^{a,b}$, $\tau_k^{b,c}$,....., $\tau_k^{y,z=a}$) is defined as:

$$\tau_k^{a,b,c,...,y,z=a} = \tau_k^{a,b}\tau_k^{b,c}...\tau_k^{y,z=a}. \tag{S77}$$

and their IRREPs are related as:

$$\begin{aligned}\Gamma(\tau_k^{a,b,c,\ldots,y,z=a}) &= \Gamma(\tau_k^{a,b}) \times \Gamma(\tau_k^{b,c}) \times \ldots \times \Gamma(\tau_k^{y,z=a}) \\ &= \Gamma(\xi_a)^2 \times \Gamma(\xi_b)^2 \\ &\times \ldots \times \Gamma(\xi_y)^2 \times \Gamma\left(\frac{\partial}{\partial R_k}\right)^N \end{aligned} \tag{S78}$$

Employing the above relation, one can find for 1D IRREPs[18]:

$$\Gamma(\tau_k^{a,b,c,\ldots,y,z=a}) = \begin{cases} \Gamma\left(\frac{\partial}{\partial R_k}\right) & \text{when } N \text{ is odd} \\ A_1' & \text{when } N \text{ is even} \end{cases} \tag{S79}$$

On the other hand, if a conical intersection (CI) point exists between two electronic states i and $i+1$, the associated electronic wavefunctions undergo sign flipping while encircling the point. Those adiabatic wavefunctions and the NACTs, $\tau_k^{i,j}$ and $\tau_k^{(i+1),j}$ belong to same IRREP (crossing-rule), which is represented as,

$$\Gamma(\tau_k^{i,j}) = \Gamma(\tau_k^{(i+1),j}). \tag{S80}$$

For Na_3 cluster, three-state SHS is created by the states $2^2E'$ and $1^2A_1'$, and there are multiple CIs within $2^2E'$ state. Hence, the second theorem leads to the following relation:

$$\begin{aligned}\Gamma(\tau_k^{1,2,3,1}) &= \Gamma(\tau_k^{12}) \times \Gamma(\tau_k^{23}) \times \Gamma(\tau_k^{31}) \\ &= \Gamma(\tau_k^{12}) \times \Gamma(\tau_k^{23})^2 \end{aligned} \tag{S81}$$

employing the conditions, $\Gamma(\tau_k^{31}) = \Gamma(\tau_k^{13})$ and $\Gamma(\tau_k^{13}) = \Gamma(\tau_k^{23})$ as per the crossing rule (Eq. S80). According to the second combination of Table S5, one can find $\Gamma(\tau_\rho^{23}) = A_1''$ and $\Gamma(\tau_\phi^{23}) = A_1'$, and hence, by using Eqs. S79 and S81, the IRREPs of τ_ρ^{12} and τ_ϕ^{12} are obtained as,

$$\begin{aligned}&\Gamma(\tau_\rho^{12}) \times (A_1'')^2 = \Gamma\left(\frac{\partial}{\partial \rho}\right) = A_2'' \\ &\Rightarrow\ \Gamma(\tau_\rho^{12}) = A_2'' \end{aligned} \tag{S82}$$

and

$$\begin{aligned}&\Gamma(\tau_\phi^{12}) \times (A_1')^2 = \Gamma\left(\frac{\partial}{\partial \phi}\right) = A_2' \\ &\Rightarrow\ \Gamma(\tau_\phi^{12}) = A_2' \end{aligned} \tag{S83}$$

When the above treatment is extended to 2D IRREP cases, we obtain the following relation for

$\Gamma(\tau_x^{23})$:[15]

$$\begin{aligned}
\Gamma(\tau_x^{23}) &= \Gamma\left(\left\langle \xi_2 \middle| \frac{\partial \xi_3}{\partial x} \right\rangle\right) \\
\Rightarrow \Gamma(\tau_x^{23}) &= \Gamma(\xi_2) \times \Gamma\left(\frac{\partial}{\partial x}\right) \times \Gamma(\xi_3) \\
\Rightarrow E' &= \Gamma(\xi_2) \times E' \times \Gamma(\xi_3). \qquad \text{(S84a)}
\end{aligned}$$

$$\text{Therefore,} \quad \Gamma(\xi_2) \times \Gamma(\xi_3) = A_1' \qquad \text{(S84b)}$$

Similarly, for $\Gamma(\tau_x^{13})$,

$$\Gamma(\xi_1) \times \Gamma(\xi_3) = A_1'. \qquad \text{(S84c)}$$

The above expressions (Eqs S84b and S84c) clearly indicate that,

$$\Gamma(\xi_1) \times \Gamma(\xi_2) \times \Gamma(\xi_3) = A_1'. \qquad \text{(S85)}$$

Finally, we achieve the following relation using Eqs S78 and S85 for the Na_3 case:

$$\begin{aligned}
\Gamma(\tau_x^{1,2,3,1}) &= \Gamma(\xi_1)^2 \times \Gamma(\xi_2)^2 \times \Gamma(\xi_3)^2 \times \Gamma\left(\frac{\partial}{\partial x}\right)^3 \\
&= A_1' \times \Gamma\left(\frac{\partial}{\partial x}\right)^3 = \Gamma\left(\frac{\partial}{\partial x}\right)^3 = (E')^3 \qquad \text{(S86)}
\end{aligned}$$

On the other hand, we arrive from Table S5 and Eq. S81,

$$\begin{aligned}
\Gamma(\tau_x^{1,2,3,1}) &= \Gamma(\tau_x^{12}) \times \Gamma(\tau_x^{23})^2 \\
&= \Gamma(\tau_x^{12}) \times (E')^2 \qquad \text{(S87)}
\end{aligned}$$

and then, by comparing Eqs. S86 and S87, one obtain $\Gamma(\tau_x^{12}) = E'$ and similarly, $\Gamma(\tau_y^{12}) = E'$. The IRREPs for all kind of NACTs for Na_3 cluster[15,22] are depicted in Table S6.

Table S6: Extended character table of molecular symmetry group $D_{3h}(M)$ with different NAC elements. This table is taken from Ref. [15].

$D_{3h}(M)$	E	(123) (132)	(12) (13) (23)	$E^\star$	$(123)^\star$ $(132)^\star$	$(12)^\star$ $(13)^\star$ $(23)^\star$	coord.	deriv.	τ_k^{23} τ_k^{13}	τ_k^{12}
A_1'	1	1	1	1	1	1			τ_ϕ	
A_2'	1	1	-1	1	1	-1	ϕ	$\frac{\partial}{\partial\phi}$		τ_ϕ
E'	2	-1	0	2	-1	0	x, y	$\frac{\partial}{\partial x}$, $\frac{\partial}{\partial y}$	τ_x,τ_y	τ_x,τ_y
A_1''	1	1	1	-1	-1	-1			τ_ρ	
A_2''	1	1	-1	-1	-1	1	ρ	$\frac{\partial}{\partial\rho}$		τ_ρ
E''	2	-1	0	-2	1	0				

S7 Extended Born-Oppenheimer (EBO) Formalism for Two and Three Electronic State Sub-Hilbert Space

S7.1 Two Electronic State Sub-Hilbert Space: Abelian Case

The nonadiabatic coupling matrix (NACM), $\boldsymbol{\tau}$ for a two electronic state sub-Hilbert space is given by,

$$\boldsymbol{\tau} = \begin{pmatrix} 0 & \boldsymbol{\tau}^{12} \\ -\boldsymbol{\tau}^{12} & 0 \end{pmatrix} = \boldsymbol{\tau}^{12} \begin{pmatrix} 0 & 1 \\ -1 & 0 \end{pmatrix} \tag{S88}$$

where $\boldsymbol{\tau}^{12} = -\boldsymbol{\nabla}_R \Theta_{12}$ and curl $\boldsymbol{\tau} = \mathbf{0}$ for any arbitrary nuclear geometry (Abelian case). Hence, one can express $\boldsymbol{\tau}$ as a product of a vector function and an antisymmetric scalar matrix. As a consequence, single-surface EBO equations can be formulated in terms of the eigenvalues of NACM, $\pm i\boldsymbol{\omega}$ $[\omega = |\boldsymbol{\tau}^{12}| = (\nabla_p \Theta_{12}^2 + \nabla_q \Theta_{12}^2 + ...)^{1/2}]$, where Θ_{12} is the nuclear coordinate dependent mixing angle between the two electronic states.

S7.2 Three Electronic State Sub-Hilbert Space: Non-Abelian Case[14]

While considering a three state sub-Hilbert space, the elements of NACM ($\boldsymbol{\tau}^{ij} = \langle\xi_i|\boldsymbol{\nabla}_R\xi_j\rangle$) are formulated as functions of ADT angles,

$$\boldsymbol{\tau}^{12} = -\cos\Theta_{13}\cos\Theta_{23}\boldsymbol{\nabla}_R\Theta_{12} - \sin\Theta_{23}\boldsymbol{\nabla}_R\Theta_{13} \tag{S89a}$$

$$\boldsymbol{\tau}^{13} = \cos\Theta_{13}\sin\Theta_{23}\boldsymbol{\nabla}_R\Theta_{12} - \cos\Theta_{23}\boldsymbol{\nabla}_R\Theta_{13} \tag{S89b}$$

$$\boldsymbol{\tau}^{23} = -\sin\Theta_{13}\boldsymbol{\nabla}_R\Theta_{12} - \boldsymbol{\nabla}_R\Theta_{23} \tag{S89c}$$

which lead to the following expressions of curl $\boldsymbol{\tau}$:

$$\begin{aligned}
\text{curl}\,\tau^{12}_{pq} = [\tau\times\tau]^{12}_{pq} &= \sin\Theta_{13}\cos\Theta_{23}(\nabla_p\Theta_{12}\nabla_q\Theta_{13} - \nabla_q\Theta_{12}\nabla_p\Theta_{13}) \\
&+ \sin\Theta_{23}\cos\Theta_{13}(\nabla_p\Theta_{12}\nabla_q\Theta_{23} - \nabla_q\Theta_{12}\nabla_p\Theta_{23}) \\
&- \cos\Theta_{23}(\nabla_p\Theta_{13}\nabla_q\Theta_{23} - \nabla_q\Theta_{13}\nabla_p\Theta_{23}) \qquad \text{(S90a)} \\
\text{curl}\,\tau^{13}_{pq} = [\tau\times\tau]^{13}_{pq} &= -\sin\Theta_{13}\sin\Theta_{23}(\nabla_p\Theta_{12}\nabla_q\Theta_{13} - \nabla_q\Theta_{12}\nabla_p\Theta_{13}) \\
&+ \cos\Theta_{23}\cos\Theta_{13}(\nabla_p\Theta_{12}\nabla_q\Theta_{23} - \nabla_q\Theta_{12}\nabla_p\Theta_{23}) \\
&+ \sin\Theta_{23}(\nabla_p\Theta_{13}\nabla_q\Theta_{23} - \nabla_q\Theta_{13}\nabla_p\Theta_{23}) \qquad \text{(S90b)} \\
\text{curl}\,\tau^{23}_{pq} = [\tau\times\tau]^{23}_{pq} &= -\cos\Theta_{13}(\nabla_p\Theta_{12}\nabla_q\Theta_{13} - \nabla_q\Theta_{12}\nabla_p\Theta_{13}), \qquad \text{(S90c)}
\end{aligned}$$

where p and q represent any two Cartesian coordinates.

While considering parametric representation of vector equation of a conical surface, the Jacobian appears as zero (0)[14,16,23,24] at those CI point(s) (see Fig. S8). Hence, the relation, curl $\boldsymbol{\tau} \simeq \mathbf{0}$ holds at the close vicinity of CI point(s) for sub-Hilbert spaces, N≥3 leading to the following relationships among the ADT angles from Eq. S90:

$$\left(\frac{\nabla_p\Theta_{13}}{\nabla_p\Theta_{12}}\right) = \left(\frac{\nabla_q\Theta_{13}}{\nabla_q\Theta_{12}}\right) \quad \text{and} \quad \left(\frac{\nabla_p\Theta_{23}}{\nabla_p\Theta_{12}}\right) = \left(\frac{\nabla_q\Theta_{23}}{\nabla_q\Theta_{12}}\right) \tag{S91}$$

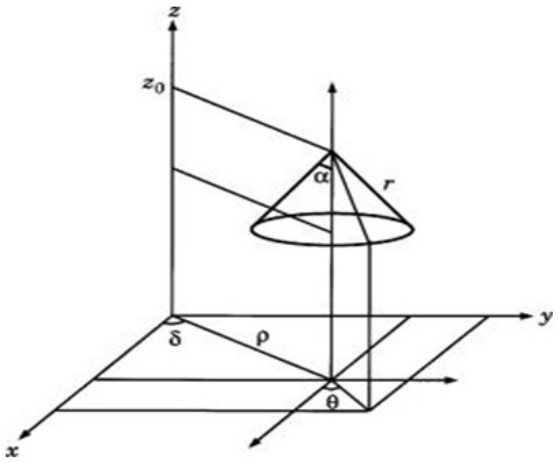

Fig. S8: The diagram portrays the conical surface over which the Jacobian Transformation is defined.[24]

While substituting the above relations in Eq. S89, we come to the following product form of NACM,

$$\boldsymbol{\tau} = \boldsymbol{\nabla}_R \Theta_{12} \begin{pmatrix} 0 & -\sin\Theta_{23}\left(\frac{\nabla_p\Theta_{13}}{\nabla_p\Theta_{12}}\right) - \cos\Theta_{13}\cos\Theta_{23} & -\cos\Theta_{23}\left(\frac{\nabla_p\Theta_{13}}{\nabla_p\Theta_{12}}\right) + \cos\Theta_{13}\sin\Theta_{23} \\ \sin\Theta_{23}\left(\frac{\nabla_p\Theta_{13}}{\nabla_p\Theta_{12}}\right) + \cos\Theta_{13}\cos\Theta_{23} & 0 & -\sin\Theta_{13} - \left(\frac{\nabla_p\Theta_{23}}{\nabla_p\Theta_{12}}\right) \\ \cos\Theta_{23}\left(\frac{\nabla_p\Theta_{13}}{\nabla_p\Theta_{12}}\right) - \cos\Theta_{13}\sin\Theta_{23} & \sin\Theta_{13} + \left(\frac{\nabla_p\Theta_{23}}{\nabla_p\Theta_{12}}\right) & 0 \end{pmatrix} \tag{S92}$$

with eigenvalues, $-i\boldsymbol{\omega}$, 0, $i\boldsymbol{\omega}$, where

$$\boldsymbol{\omega} = \boldsymbol{\nabla}_R \Theta_{12} \left[1 + \left(\frac{\nabla_p\Theta_{13}}{\nabla_p\Theta_{12}}\right)^2 + \left(\frac{\nabla_p\Theta_{23}}{\nabla_p\Theta_{12}}\right)^2 + 2\sin\Theta_{13}\left(\frac{\nabla_p\Theta_{23}}{\nabla_p\Theta_{12}}\right)\right]^{1/2}. \tag{S93}$$

S8 Even-Parity PESs and Couplings for Asymmetric Stretching/Bending Modes

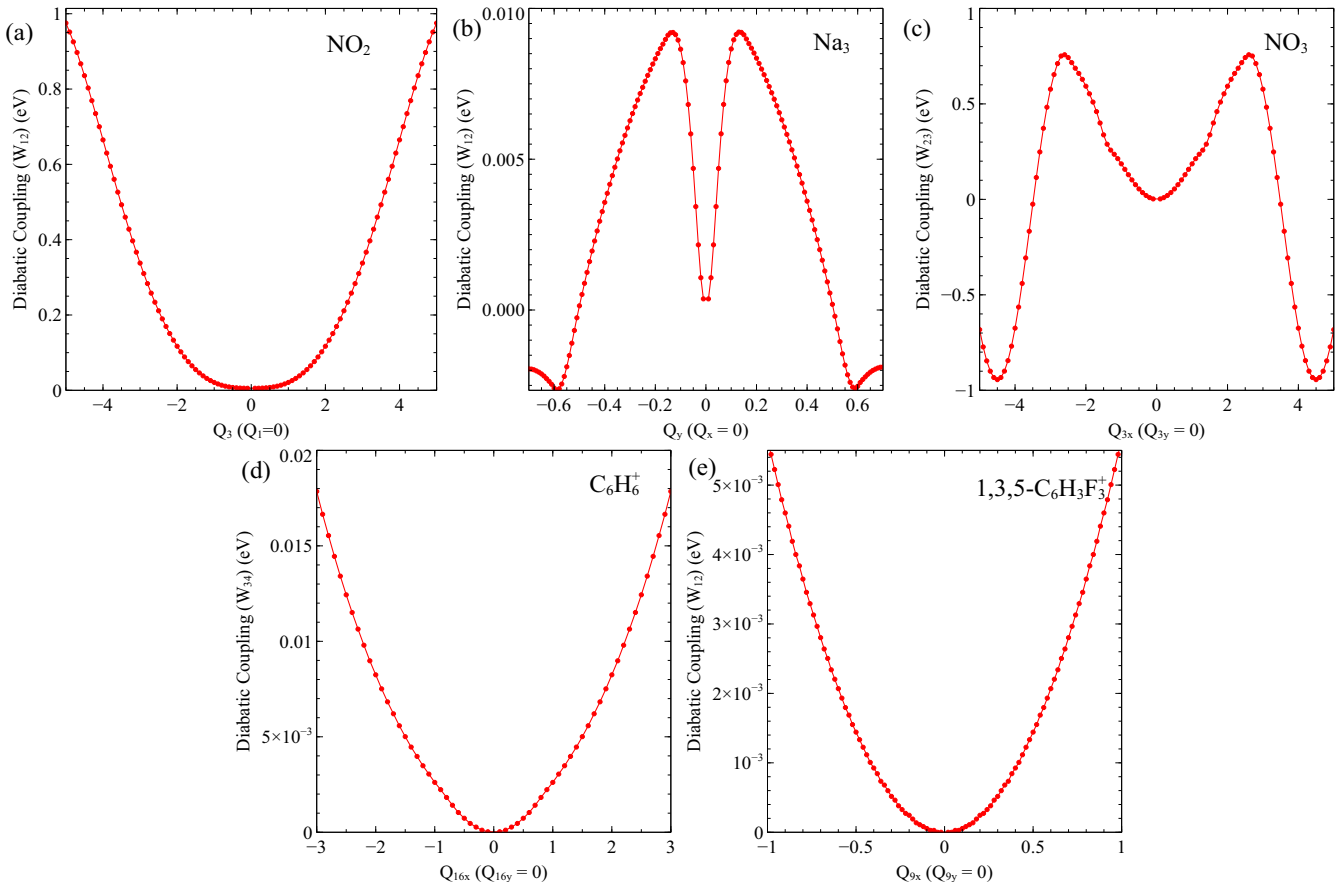

Fig. S9: The upper panel [(a) - (c)] depicts 1D cuts of diabatic coupling elements, W_{12} of NO_2 radical (X^2A_1 and A^2B_2) along Q_3, W_{12} of Na_3 cluster ($2\,^2E'$) along Q_y and W_{23} of NO_3 radical ($\tilde{A}^2E''$) along Q_{3x} mode, respectively. On the other hand, the lower panel [(d) and (e)] represents 1D variation of diabatic couplings, W_{34} of $C_6H_6^+$ ($\tilde{B}^2E_{2g}$) along Q_{16x} and W_{12} of 1,3,5-$C_6H_3F_3^+$ radical cation ($\tilde{X}^2E''$) along Q_{9x} normal mode, respectively. In all cases, the couplings show symmetric functional forms, which can be fitted with even power polynomials.

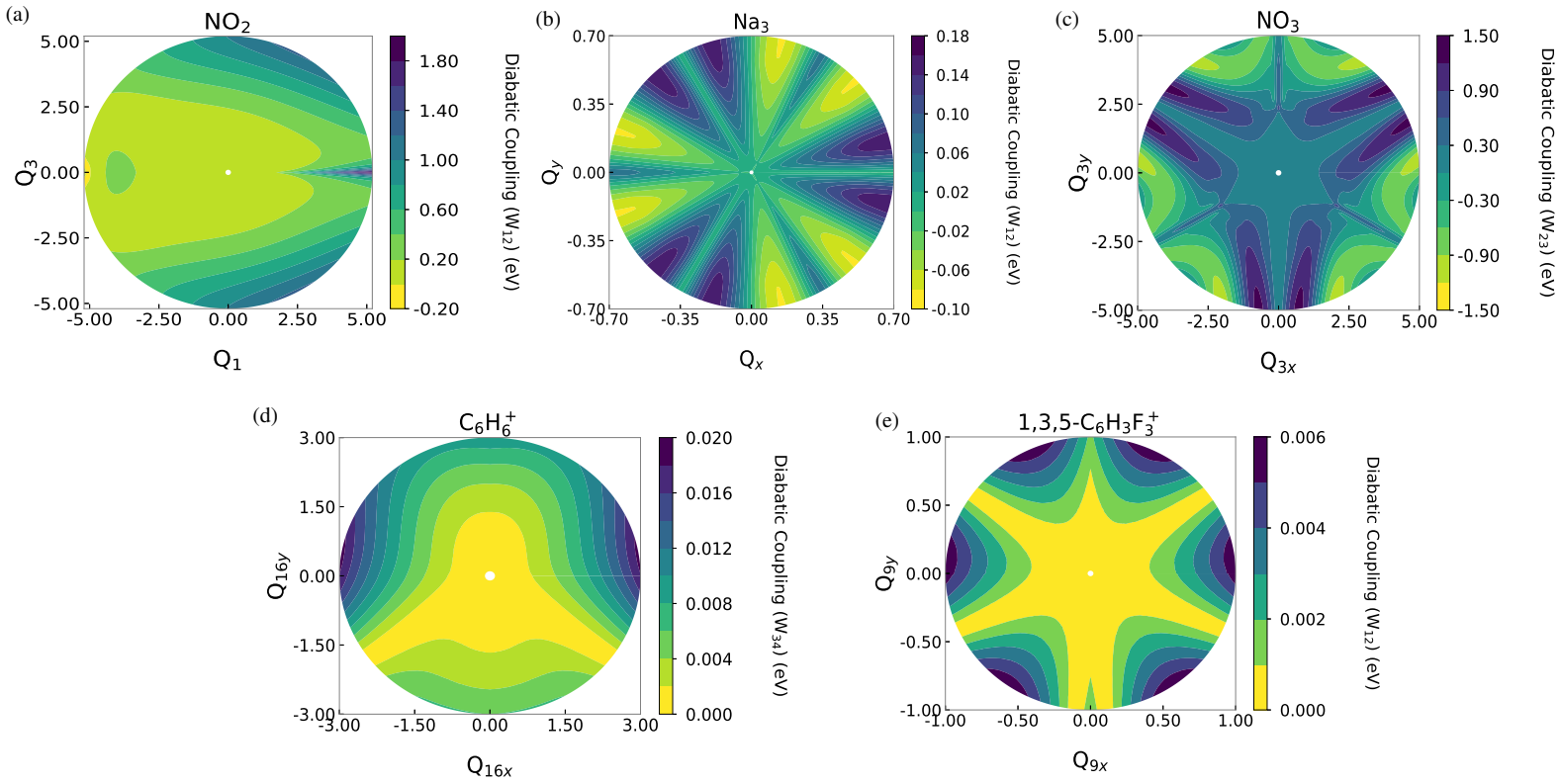

Fig. S10: The above diagram demonstrates 2D contour of diabatic coupling elements, namely, (a) W_{12} of NO_2 radical (X^2A_1 and A^2B_2) over $Q_1 - Q_3$ plane, (b) W_{12} of Na_3 cluster ($2\,^2E'$) over $Q_x - Q_y$ plane, (c) W_{23} of NO_3 radical ($\tilde{A}^2E''$) over $Q_{3x} - Q_{3y}$ nuclear plane, (d) W_{34} of $C_6H_6^+$ ($\tilde{B}^2E_{2g}$) over $Q_{16x} - Q_{16y}$ plane and (e) W_{12} of 1,3,5-$C_6H_3F_3^+$ ($\tilde{X}^2E''$) over $Q_{9x} - Q_{9y}$ plane. It is clearly evident that the couplings exhibit symmetric functional variation along Q_3, Q_y, Q_{3x}, Q_{16x} and Q_{9x} normal modes of NO_2, Na_3, NO_3, $C_6H_6^+$ and 1,3,5-$C_6H_3F_3^+$, respectively.

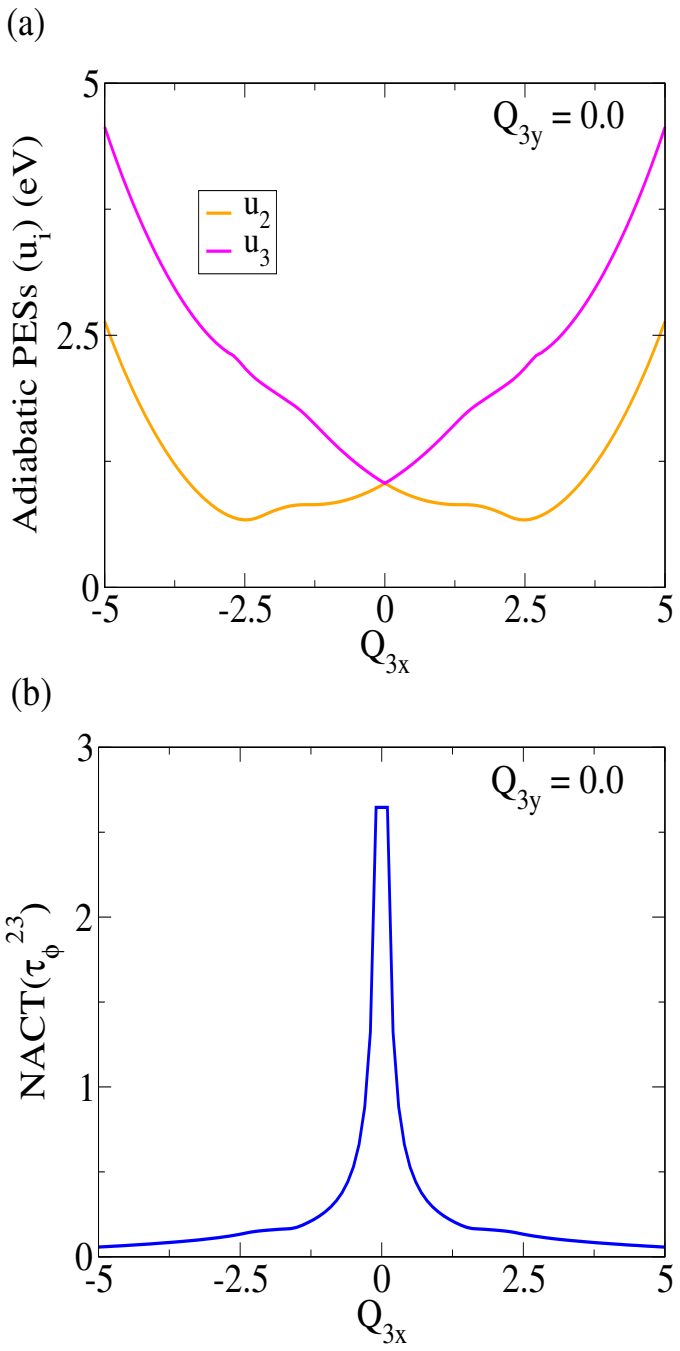

Fig. S11: Panel (a) portrays adiabatic potential energy curves (PECs), u_2 and u_3 ($\tilde{A}^2E''$) as function of Q_{3x} normal mode of NO_3 radical keeping the magnitude of Q_{3y} at zero (0). On the other hand, panel (b) depicts 1D variation of ϕ component of associate NACT (τ_ϕ^{23}) along the same coordinate (Q_{3x}). In both the situations, the curves exhibit symmetric functional form along Q_{3x} coordinate and thereby, the corresponding diabatic coupling (W_{23}) also shows such symmetric variation (see Fig. S9c and S10c).

S9 Calculation of Theoretical Photodetachment Spectra

While performing nuclear dynamics to simulate photodetachment spectra of prototypical molecular systems with FFT-Lanczos or time-dependent discrete variable representation (TDDVR) methodology, the time-dependent SE is solved to compute the nuclear wavefunctions [$\boldsymbol{\psi}(t)$] at different time. These wavefunctions are employed to evaluate the following autocorrelation function:

$$C(t) = \langle \boldsymbol{\psi}(0) | \boldsymbol{\psi}(t) \rangle, \tag{S94}$$

$$= \langle \boldsymbol{\psi}^{\star}(t/2) \, | \boldsymbol{\psi}(t/2) \rangle. \tag{S95}$$

It is important to highlight that Eq. S95 is more accurate and computationally faster for implementation than the other one (Eq. S94), though Eq. S95 is applicable only for real initial wavefunction and the Hamiltonian is totally symmetric (A_1). Those functions (Eq. S95) are used to carry out the following Fourier transformation,

$$I(\omega) \propto \omega \int_{-\infty}^{\infty} C(t) \exp(i\omega t) dt, \tag{S96}$$

where ω is frequency and $I(\omega)$ dictates the intensity of the spectral bands in the photodetachment spectra of a molecule.

S10 Implementation of Beyond Born-Oppenheimer (BBO) Theory on Model Hamiltonian of Na_3 Cluster[25,26]

In order to explore the validity of EBO formalism for a tri-state system, we have selectively chosen the model form of diabatic Hamiltonian for Na_3 cluster proposed by Cocchini *et al.*[25] In this system, $2\,^2E'$ and $1\,^2A_1'$ states are nonadiabatically coupled over the nuclear plane constituted with polar counterparts ($\rho - \phi$) of bending (Q_x) and asymmetric stretching (Q_y) modes. The model diabatic Hamiltonian is:[25]

$$V^{\text{dia}}(\rho, \phi) = \begin{pmatrix} \frac{\rho^2}{2} + U_2 & U_1 & W_1 - W_2 \\ U_1 & \frac{\rho^2}{2} - U_2 & W_1 + W_2 \\ W_1 - W_2 & W_1 + W_2 & \epsilon_0 + \frac{\rho^2}{2} \end{pmatrix}, \tag{S97}$$

where

$$U_1(\rho,\phi) = K\rho\cos\phi + \frac{1}{2}g\rho^2\cos(2\phi) \qquad W_1(\rho,\phi) = P\rho\cos\phi + \frac{1}{2}f\rho^2\cos(2\phi)$$
$$U_2(\rho,\phi) = K\rho\sin\phi - \frac{1}{2}g\rho^2\sin(2\phi) \qquad W_2(\rho,\phi) = P\rho\sin\phi - \frac{1}{2}f\rho^2\sin(2\phi)$$

In the above expressions, JT coupling constants [K (= 4.9) and g (= 0.035)][25] and PJT coupling parameters [P (= 3.46) and f (= 0.025)][25] appear in dimensionless units as the nuclear coordinates are dimensionless. On the other hand, the adjustable parameter, ϵ_0 (= 2Δ) dictates the energy separation (Δ) between second and third states.

At the PJT situation ($K = g = 0$), analytic expressions of ρ and ϕ components of NACTs can be calculated analytically from the diabatic Hamiltonian (Eq. S97) as:

$$\tau_\rho^{12} = -\frac{A_0}{\sqrt{2wB_-}}, \quad \tau_\rho^{13} = -\frac{A_0}{\sqrt{2wB_+}}, \quad \tau_\rho^{23} = \frac{A_1\Delta}{2\sqrt{2w}(\Delta^2+2w)}, \tag{S98a}$$
$$\tau_\phi^{12} = \frac{A_2}{\sqrt{2wB_-}}, \quad \tau_\phi^{13} = \frac{A_2}{\sqrt{2wB_+}}, \quad \tau_\phi^{23} = -\frac{3\rho A_0\Delta}{2\sqrt{2w}(\Delta^2+2w)}, \tag{S98b}$$

where

$$A_0(\rho,\phi) = Pf\rho^2\sin(3\phi)$$
$$A_1(\rho,\phi) = 2P^2\rho + f^2\rho^3 + 3Pf\rho^2\cos(3\phi)$$
$$A_2(\rho,\phi) = 2P^2\rho^2 - f^2\rho^4 - Pf\rho^3\cos(3\phi)$$
$$B_\pm(\rho,\phi) = 2w + (\Delta \pm \sqrt{\Delta^2+2w})^2$$
$$w(\rho,\phi) = W_1^2 + W_2^2 = P^2\rho^2 + \frac{f^2\rho^4}{4} + Pf\rho^3\cos(3\phi)$$

Again, the curls take the following analytical forms:

$$\text{curl}\,\tau_{\rho\phi}^{12} = -\frac{(3\rho A_0^2 - A_1A_2)\Delta}{4w(\Delta^2+2w)\sqrt{B_+}}; \quad \text{curl}\,\tau_{\rho\phi}^{13} = \frac{(3\rho A_0^2 - A_1A_2)\Delta}{4w(\Delta^2+2w)\sqrt{B_-}}; \quad \text{curl}\,\tau_{\rho\phi}^{23} = 0. \tag{S99}$$

It is evident from the above functional forms that curl $\tau_{\rho\phi}^{ij}$s become identically zero (0) at $\Delta = 0$, i.e., at the point of three-state degeneracy between A and E states. On the other hand, the numerically calculated curls obtained from gradient of ADT angles appear to be negligibly small (curl $\tau_{\rho\phi}^{ij} \approx 0$) up to certain nonzero Δ ($\leq$ 172 cm^{-1}). Hence, for $\Delta = 0$, there exists a common diagonalizing matrix, G for both the matrices (τ_ρ and τ_ϕ), which can transform the adiabatic SE (see Eq. 29 of main article) to the following form:

$$-\frac{\hbar^2}{2}\left(\boldsymbol{\nabla}_R+\boldsymbol{\Omega}\right)^2\Phi+\left(V-E\right)\Phi=0, \tag{S100}$$
$$\text{where}\quad \psi^{\text{ad}}=G\Phi,\quad \boldsymbol{\Omega}=G^{\dagger}\boldsymbol{\tau}G\quad\text{and}\quad V=G^{\dagger}UG.$$

For three state degeneracy ($\Delta=0$), the diagonalizing matrix (G) is found to be

$$G=\begin{pmatrix} 0 & \frac{-i}{\sqrt{2}} & \frac{i}{\sqrt{2}} \\ \frac{-1}{\sqrt{2}} & \frac{1}{2} & \frac{1}{2} \\ \frac{1}{\sqrt{2}} & \frac{1}{2} & \frac{1}{2} \end{pmatrix}$$

When the value of Δ is low ($\leq$172 cm^{-1}), the magnitude of curl $\boldsymbol{\tau}$ is negligibly small (curl $\boldsymbol{\tau}\approx 0$) and therefore, the above formulation is approximately valid. At this junction, one can impose classical inaccessibility condition for each electronic state from others at and around a specific energy, i.e., $|\psi_i|\gg|\psi_j|$ $(i\neq j)$ and then, the single-surface EBO equations take the following form,

$$-\frac{\hbar^2}{2m}\left\{\left(\frac{\partial}{\partial\rho}+i\omega_\rho\right)^2+\frac{1}{\rho}\left(\frac{\partial}{\partial\rho}+i\omega_\rho\right)+\frac{1}{\rho^2}\left(\frac{\partial}{\partial\phi}+i\omega_\phi\right)^2\right\}\Phi_1+(u_1-E)\Phi_1=0, \tag{S101a}$$
$$-\frac{\hbar^2}{2m}\left\{\frac{\partial^2}{\partial\rho^2}+\frac{1}{\rho}\frac{\partial}{\partial\rho}+\frac{1}{\rho^2}\frac{\partial^2}{\partial\phi^2}\right\}\Phi_2+(u_2-E)\Phi_2=0, \tag{S101b}$$
$$-\frac{\hbar^2}{2m}\left\{\left(\frac{\partial}{\partial\rho}-i\omega_\rho\right)^2+\frac{1}{\rho}\left(\frac{\partial}{\partial\rho}-i\omega_\rho\right)+\frac{1}{\rho^2}\left(\frac{\partial}{\partial\phi}+i\omega_\phi\right)^2\right\}\Phi_3+(u_3-E)\Phi_3=0, \tag{S101c}$$

where u_1, u_2 and u_3 are adiabatic PESs, and ω_ρ and ω_ϕ are the two components of NACM eigenvalues. The angular component, ω_ϕ $(=\frac{A_2}{2w})$ appears to be gauge invariant ($\int_0^{2\pi}\omega_\phi d\phi=2\pi$) for three state degeneracy, which in turn affirms the workability of the EBO equations (Eq. S101) over the specific domain of nuclear configuration space (CS).

We have generated the photoabsorption spectra for the lower sheet of E' state of Na_3 cluster employing ordinary BO, EBO (Eq. S101a) and diabatic SEs (Eq. S97) with $\Delta=0$ and 172 cm^{-1}, which are illustrated in Subsection 8.2.1 of the main article.

S11 Formulation of Time-dependent 3D wave-packet methodology in hyperspherical coordinates

The initial wave packet is represented in terms of $3-j$ symbols and modified spherical harmonics ($C_{j\mu}$) as:

$$\begin{aligned}\Phi_K^a &= \sqrt{2\pi\ \sin\eta\ J(Rr\eta|\rho\theta\phi)(2l+1)}\phi_{vj}(r)\ \chi(R)(-1)^{j-l} \\ &\times \sum_{\mu}\begin{pmatrix} j & l & J \\ \mu & 0 & -\mu \end{pmatrix} C_{j\mu}(\eta)A_{K\mu},\end{aligned} \tag{S102}$$

where various terms carry their usual meaning.[27,28]

The diabatic Hamiltonian operator for the triatomic system is expressed in terms of Johnson's hyperspherical coordinates:[29]

$$\begin{aligned}\hat{H} &= \{-\frac{\hbar^2}{2\mu_R}\frac{\partial^2}{\partial\rho^2} + \frac{2}{\mu_R\rho^2}\hat{L}^2(\theta,\phi) \\ &+\frac{\hat{J}^2-\hat{J}_z^2}{\mu_R\rho^2\cos^2\theta} + \frac{\hat{J}_z^2 - 4\cos\theta\ \hat{J}_z\hat{P}_\phi}{2\mu_R\rho^2\sin^2\theta} \\ &+\frac{\sin\theta}{\mu_R\rho^2\cos^2\theta}\frac{1}{2}[\hat{J}_+^2+\hat{J}_-^2]\}\hat{\mathrm{I}} + \hat{V}_0(\rho,\theta,\phi),\end{aligned} \tag{S103}$$

where $\hat{V}_0(\rho,\theta,\phi)$ denotes the (3×3) interaction (diabatic) potential matrix for the triatomic system, and other operators are described elsewhere.[30] The adiabatic K-component wavefunctions ($\Phi_{K,I}^a$) for different surfaces ($I=1,2,3$) are transformed to the diabatic ones ($\Phi_{K,I}^d$) by using the matrix that diagonalizes $\hat{V}_0(\rho,\theta,\phi)$. Thereafter, we obtain the following set of coupled equations in terms of K-component waves ($\Phi_{K,I}^d$) for all the three surfaces:

$$\begin{aligned}i\hbar\frac{\partial}{\partial t}\begin{bmatrix}\Phi_{K,1}^d \\ \Phi_{K,2}^d \\ \Phi_{K,3}^d\end{bmatrix} =& \Big\{ -\frac{\hbar^2}{2\mu_R}\frac{\partial^2}{\partial\rho^2} + \frac{2}{\mu_R\rho^2}\hat{L}^2(\theta,\phi) \\ &+\frac{\hbar K(\hbar K - 4\cos\theta\ \hat{P}_\phi)}{2\mu_R\rho^2\ \sin^2\theta} + \frac{\hbar^2[J(J+1)-K^2]}{\mu_R\rho^2\cos^2\theta} \\ &+\Delta V(\rho,\theta)\Big\}\begin{bmatrix}\Phi_{K,1}^d \\ \Phi_{K,2}^d \\ \Phi_{K,3}^d\end{bmatrix}\end{aligned}$$

$$
+\begin{bmatrix} V_{11}+\Delta V & V_{12} & V_{13} \\ V_{21} & V_{22}+\Delta V & V_{23} \\ V_{31} & V_{32} & V_{33}+\Delta V \end{bmatrix}
\begin{bmatrix} \Phi^d_{K,1} \\ \Phi^d_{K,2} \\ \Phi^d_{K,3} \end{bmatrix}
$$

$$
+\frac{\sin\theta}{\mu_R \rho^2 \cos^2\theta}\left(M_{K,K+2}\begin{bmatrix} \Phi^d_{K+2,1} \\ \Phi^d_{K+2,2} \\ \Phi^d_{K+2,3} \end{bmatrix} \right.
$$

$$
\left. +M_{K,K-2}\begin{bmatrix} \Phi^d_{K-2,1} \\ \Phi^d_{K-2,2} \\ \Phi^d_{K-2,3} \end{bmatrix} \right), \tag{S104}
$$

where two K-component diabatic wavefunctions $\Phi^d_{K,I}$ and $\Phi^d_{K\pm2,I}$ are coupled via the coupling element:

$$
M_{K,K\pm2} = \frac{\hbar^2}{2}\sqrt{(J\mp K)(J\pm K+1)(J\mp K-1)(J\pm K+2)}. \tag{S105}
$$

The time-dependent wave packet is projected[31,32] onto asymptotic eigenstates at a fixed value of R ($= R^*$) and the scattering amplitude in the channel specified by vibrational, rotational and orbital quantum numbers v', j', l' for different surfaces (I = 1, 2, 3) are obtained as:

$$
\begin{aligned}
u^{J,I}_{v'j'l'}(R^*;t) &= 4R^* \int dr \int d\eta\; r\sin\eta\; \rho^{-5/2}(\sin 2\theta)^{-1/2}\phi^I_{v'j'}(r) \\
&\times \sum_{K\mu'} g_{j'l'\mu'} A^*_{K\mu'} C_{j'\mu'}(\eta)\Phi^a_{K,I}(\rho,\theta,\phi),
\end{aligned} \tag{S106}
$$

where at each step of the time propagation, the diabatic K-component wavefunctions ($\Phi^d_{K,I}$) are transformed back to the adiabatic ones ($\Phi^a_{K,I}$)[28,30] for analysing the wavefunction.

Thereafter, the scattering amplitudes are Fourier transformed from time to energy domain after the wave packet passes through the projection region and gets almost absorbed at the boundary.

$$
b^{J,I}_{v'j'l'}(E;R) = \frac{1}{\sqrt{2\pi}}\int dt\; u^{J,I}_{v'j'l'}(R;t)\exp(iEt/\hbar). \tag{S107}
$$

Those amplitudes are expanded in terms of incoming and outgoing waves as:

$$
b^{J,I}_{v'j'l'} = A^{in}_{v'j'l'} k_{v'j'} R\; h^-(k_{v'j'}R) + A^{out,I}_{v'j'l'} k_{v'j'} R\; h^+(k_{v'j'}R), \tag{S108}
$$

where

$$h^{\pm}(k_{v'j'}R) = -n_l(k_{v'j'}R) \pm ij_l(k_{v'j'}R), \tag{S109}$$

with j_l and n_l being spherical Bessel and Neumann functions, respectively.

Moreover, we can perform a transformation from the unique adiabatic to the approximate diabatic representation to obtain the amplitudes corresponding to the asymptotic product states as:

$$\begin{aligned}
\Phi^d_{K,1} &= \Phi^a_{K,1}, & r < r_c \\
\Phi^d_{K,1} &= \Phi^a_{K,2}, & r \geq r_c \\
\Phi^d_{K,2} &= \Phi^a_{K,2}, & r < r_c \\
\Phi^d_{K,2} &= \Phi^a_{K,1}, & r \geq r_c
\end{aligned} \tag{S110}$$

where the indices 1 and 2 represent the neutral (H_2) and ionic (H_2^+) products, respectively, and the corresponding potential curves cross at r_c. Thus, the scattering amplitudes can be evaluated as:

$$\begin{aligned}
d^1_{v',j',l'} &= \sum_v \{b^{J,1}_{v,j',l'} Sl^{11}_{v,v',j'} + b^{J,2}_{v,j',l'} Sr^{21}_{v,v',j'}\}, \\
d^2_{v',j',l'} &= \sum_v \{b^{J,2}_{v,j',l'} Sl^{22}_{v,v',j'} + b^{J,1}_{v,j',l'} Sr^{12}_{v,v',j'}\},
\end{aligned} \tag{S111}$$

where Sl and Sr are coupling elements between the vibrational wavefunctions:

$$\begin{aligned}
Sl^{II'}_{v,v',j'} &= \int_0^{r_c} \phi^I_{vj'} \phi^{I'}_{v'j'}, \\
Sr^{II'}_{v,v',j'} &= \int_{r_c}^{\infty} \phi^I_{vj'} \phi^{I'}_{v'j'}.
\end{aligned} \tag{S112}$$

The state-to-state reaction probability on I^{th} surface could be calculated by taking the ratio of the outgoing and incoming fluxes:

$$P^I_{v'j'l' \leftarrow vjl} = \frac{F^I_{v'j'l'}}{F_{vjl}}, \tag{S113}$$

where

$$F^I_{v'j'l'} = \frac{1}{\mu_{out}} k_{v'j'} |d^I_{v',j',l'}|^2, \tag{S114}$$

$$F_{vjl} = \frac{1}{\mu_{in}} k_{vj} |c^l_E|^2. \tag{S115}$$

and each terms carry their usual meaning.[27] Indeed, for a Gaussian wave packet, the weight of the scattering amplitudes in energy (E) and wave vector (k) space are related as:

$$|c_E^l|^2 \quad = \quad \left(\frac{\mu_{in}}{\hbar k}\right)^2 \sqrt{2/\pi}\ A_0\ \exp[-2A_0^2(k-k_0)^2], \tag{S116}$$

with A_0 being the width of the Gaussian wavepacket.

Finally, total integral cross sections (ICSs) at a particular collision energy are evaluated by summing over the reaction probabilities of all final rovibrational states for all values of total angular momentum, J:

$$\sigma(E) = \frac{\pi}{\kappa_{vj}^2} \sum_{j'=0}^{j'_{max}} \sum_{v'=0}^{v'_{max}} \sum_{J=0}^{J_{max}} (2J+1) P^J_{v'j' \leftarrow vj}(E) \tag{S117}$$

S11.1 The absorbing potential, propagation, projection and computation details

A negative imaginary potential $[-iV_{Im}(\rho)]$ is plugged in at the last 20% - 30% of ρ - grid points for each hyperangles in order to avoid any unrealistic reflection. Therefore, the total potential can be represented as:

$$V(\rho, \theta, \phi) = V_0(\rho, \theta, \phi) - iV_{Im}(\rho)\,, \tag{S118}$$

where a linear absorbing potential[33,34] of the following form is used in our present calculations:

$$V_{Im}(\rho) = \begin{cases} V_{opt} \cdot (\rho - \rho_I), & \rho_I \leq \rho \\ 0, & \text{otherwise,} \end{cases}$$

where V_{opt} controls minimum reflection from the boundary and ρ_I is the starting point of the absorbing potential. The various parameters employed in our dynamical calculations are depicted in Table S7.

The intrinsically parallel version of the Fast Fourier Transformation (FFT)[35] algorithm is utilized to evaluate the kinetic energy operators, which efficiently scales the computational cost as $cN \log N$, with N being the total number of grid points in hyperspherical coordinates. While evaluating the kinetic energy operators on the wavefunction by FFT routine, the θ range is extended from $\pi/2$ to π and the associated amplitudes on the grid points are taken as reverse mirror image of those from 0 to $\pi/2$ making the resulting function an odd function around $\theta = \pi/2$. This extension of the

domain of θ leads to sine transformation, where the amplitudes of the wavefunction automatically become zero at $\theta = 0$, $\pi/2$ and π. On the other hand, time propagation of the wave packet is performed by using iterative Lanczos reduction technique.[36] Moreover, we have implemented mixed Open Multi-Processing (OpenMP) - Massage Passing Interface (MPI) parallelization scheme,[28,30] which helps to overcome the huge computational demand.

Table S7: Dynamical parameters for initialization, projection, and absorbing potential: $v = 0, j = 0; J = 0, 1, 2, ..., 34$. [The numbers in the parenthesis are the corresponding transformed values in ρ - space.]

Grid size:	
N_ρ	256
N_θ	64
N_ϕ	128
(ρ_{min}, ρ_{max})/Å	(1.0, 10.0)
Translational wave packet:	
R_0/Å	5.50 ($\sim$ 6.56)
R_f/Å	1.70 ($\sim$ 2.75)
A_0/Å	0.20
k_0 (Å^{-1})	36.3523
Rovibrational energy:	
E_{vj} (eV)	0.269763
Propagation:	
Δ t (fs)	0.050
Magnitude of the normalized five last Lanczos vectors	$10^{-8} - 10^{-7}$
Absorbing potential:	
V_{opt}/eV	0.163
ρ_I (Å)	8.0
Range of the absorbing potential (Å)	8.0 - 10.0
Projection:	
R* (Å)	5.25 ($\sim$ 6.45)
vib. states	$v' = 0, \cdots, 10$
rot. states	$j' = 0, \cdots, 12$

References

[1] M. Born and J. R. Oppenheimer, *Ann. Phys. (Leipzig)*, 1927, **84**, 457–84.

[2] M. Born and K. Huang, *Dynamical Theory of Crystal Lattices*, Oxford University Press, Oxford, 1954.

[3] H. A. Jahn and E. Teller, *Proc. Roy. Soc. (London)*, 1937, **161**, 220–35.

[4] U. Öpik and M. H. L. Pryce, *Proc. R. Soc. London, Ser. A*, 1957, **238**, 425–447.

[5] H. C. Longuet-Higgins, U. Öpik, M. H. L. Pryce and R. A. Sack, *Proc. R. Soc. London, Ser. A*, 1958, **244**, 1–16.

[6] J. Dutta, S. Adhikari and N. Kovaleva, *J. Chem. Phys.*, 2019, **150**, 064703.

[7] M. C. M. O'Brien, *Proc. Roy. Soc. A*, 1964, **281**, 323.

[8] N. N. Kovaleva, O. E. Kusmartseva, K. I. Kugel, A. A. Maksimov, D. Nuzhnyy, A. M. Balbashov, E. I. Demikhov, A. Dejneka, V. A. Trepakov, F. V. Kusmartsev and A. M. Stoneham, *J. Phys.: Condens. Matter*, 2013, **25**, 155602.

[9] N. N. Kovaleva, O. E. Kusmartseva, K. I. Kugel and F. V. Kusmartsev, *J. Phys.: Conf. Ser.*, 2017, **833**, 012005.

[10] J. Rodríguez-Carvajal, M. Hennion, F. Moussa, A. H. Moudden, L. Pinsard and A. Revcolevschi, *Phys. Rev. B*, 1998, **57**, R3189.

[11] J. C. Slonczewski, *Phys. Rev.*, 1963, **131**, 1596.

[12] J. H. V. Vleck, *J. Chem. Phys.*, 1939, **7**, 72–84.

[13] Z. H. Top and M. Baer, *J. Chem. Phys.*, 1977, **66**, 1363.

[14] B. Sarkar and S. Adhikari, *J. Chem. Phys.*, 2006, **124**, 074101.

[15] S. Mukherjee, S. Bandyopadhyay, A. K. Paul and S. Adhikari, *J. Phys. Chem. A*, 2013, **117**, 3475–95.

[16] B. Sarkar and S. Adhikari, *J. Phys. Chem. A*, 2008, **112**, 9868–85.

[17] S. Mukherjee, B. Mukherjee and S. Adhikari, *J. Phys. Chem. A*, 2017, **121**, 6314–26.

[18] S. Al-Jabour, M. Baer, O. Deeb, M. Leibscher, J. Manz, X. Xu and S. Zilberg, *J. Phys. Chem. A*, 2010, **114**, 2991–3010.

[19] S. F. A. Kettle, *Symmetry and Structure: Readable Group Theory for Chemists: 3rd edition*, J. Wiley and Sons Inc: West Sussex, England, 2007.

[20] P. R. Bunker and P. Jensen, *Molecular symmetry and spectroscopy: 2nd edition*, NRC Research Press, 2006.

[21] T. Vértesi, A. Vibók, G. J. Halász and M. Baer, *J. Chem. Phys.*, 2004, **120**, 2565.

[22] S. Mukherjee and S. Adhikari, *Chem. Phys.*, 2014, **440**, 106–18.

[23] S. Mukherjee, B. Mukherjee, S. Sardar and S. Adhikari, *Comp. Theor. Chem.*, 2019, **1154**, 57–67.

[24] D. J. Griffiths, *Introduction to Electrodynamics*, Prentice-Hall, Englewood Cliffs, NJ, 1989.

[25] F. Cocchini, T. H. Upton and W. Andreoni, *J. Chem. Phys.*, 1988, **88**, 6068–77.

[26] A. K. Paul, S. Sardar, B. Sarkar and S. Adhikari, *J. Chem. Phys.*, 2009, **131**, 124312.

[27] S. Adhikari and A. J. C. Varandas, *Comput. Phys. Comm.*, 2013, **184**, 270–83.

[28] S. Ghosh, T. Sahoo, S. Adhikari, R. Sharma and A. J. C. Varandas, *J. Phys. Chem. A*, 2015, **119**, 12392.

[29] B. R. Johnson, *J. Chem. Phys.*, 1983, **79**, 1916–1925.

[30] S. Ghosh, S. Mukherjee, B. Mukherjee, S. Mandal, R. Sharma, P. Chaudhury and S. Adhikari, *J. Chem. Phys.*, 2017, **147**, 074105.

[31] G. D. Billing and N. Markovic, *J. Chem. Phys.*, 1993, **99**, 2674–9.

[32] G. D. Billing and N. Markovic, *J. Chem. Phys.*, 1994, **100**, 1085.

[33] D. Neuhasuer and M. Baer, *J. Chem. Phys.*, 1989, **90**, 4351.

[34] N. Markovic and G. D. Billing, *Chem. Phys.*, 1995, **191**, 247–260.

[35] D. Kosloff and R. Kosloff, *J. Comput. Phys.*, 1986, **52**, 35–53.

[36] T. J. Park and J. C. Light, *J. Chem. Phys.*, 1986, **85**, 5870–5876.